



Localized rest and stress human cardiac creatine kinase reaction kinetics at 3 tesla

Journal:	<i>NMR in Biomedicine</i>
Manuscript ID	NBM-18-0258.R2
Wiley - Manuscript type:	Research Article
Date Submitted by the Author:	24-Jan-2019
Complete List of Authors:	<p>Clarke, William; University of Oxford, Wellcome Centre for Integrative Neuroimaging, FMRIB, Nuffield Department of Clinical Neurosciences; University of Oxford, Oxford Centre for Clinical Magnetic Resonance Research(OCMR), Division of Cardiovascular Medicine RDM</p> <p>Peterzan, Mark; University of Oxford, Oxford Centre for Clinical Magnetic Resonance Research(OCMR), Division of Cardiovascular Medicine RDM</p> <p>Rayner, Jennifer; University of Oxford, Oxford Centre for Clinical Magnetic Resonance Research(OCMR), Division of Cardiovascular Medicine RDM</p> <p>Sayeed, Rana; Oxford University Hospitals NHS Foundation Trust, Department of Cardiothoracic Surgery, John Radcliffe Hospital</p> <p>Petrou, Mario; Oxford University Hospitals NHS Foundation Trust, Department of Cardiothoracic Surgery, John Radcliffe Hospital</p> <p>Krasopoulos, George; Oxford University Hospitals NHS Foundation Trust, Department of Cardiothoracic Surgery, John Radcliffe Hospital</p> <p>Lake, Hannah; University of Oxford, Department of Cardiovascular Medicine, Wellcome Trust Centre for Human Genetics</p> <p>Raman, Betty; University of Oxford, Oxford Centre for Clinical Magnetic Resonance Research(OCMR), Division of Cardiovascular Medicine RDM</p> <p>Watson, William; University of Oxford, Oxford Centre for Clinical Magnetic Resonance Research(OCMR), Division of Cardiovascular Medicine RDM</p> <p>Cox, Pete; University of Oxford, Department of Physiology Anatomy</p> <p>Hundertmark, Mortiz; University of Oxford, Oxford Centre for Clinical Magnetic Resonance Research(OCMR), Division of Cardiovascular Medicine RDM</p> <p>Apps, Andrew; University of Oxford, Oxford Centre for Clinical Magnetic Resonance Research(OCMR), Division of Cardiovascular Medicine RDM</p> <p>Lygate, Craig; University of Oxford, Department of Cardiovascular Medicine, Wellcome Trust Centre for Human Genetics</p> <p>Neubauer, Stefan; University of Oxford, Oxford Centre for Clinical Magnetic Resonance Research(OCMR), Division of Cardiovascular Medicine RDM</p> <p>Rider, Oliver; University of Oxford, Oxford Centre for Clinical Magnetic Resonance Research</p> <p>Rodgers, Christopher (Chris); University of Cambridge Department of Physiology Development and Neuroscience, Wolfson Brain Imaging Centre; University of Oxford, Oxford Centre for Clinical Magnetic Resonance Research(OCMR), Division of Cardiovascular Medicine RDM</p>

1
2
3
4
5
6
7
8
9
10
11
12
13
14
15
16
17
18
19
20
21
22
23
24
25
26
27
28
29
30
31
32
33
34
35
36
37
38
39
40
41
42
43
44
45
46
47
48
49
50
51
52
53
54
55
56
57
58
59
60

Keywords:	Phosphorus MRS/MRSI < MR Spectroscopy (MRS) and Spectroscopic Imaging (MRSI) Methods < Methods and Engineering, Human study < Cardiovascular < Applications, Heart function < Cardiovascular MR (CMR) Methods < Methods and Engineering, MR Spectroscopy (MRS) and Spectroscopic Imaging (MRSI) Methods < Methods and Engineering

SCHOLARONE™
Manuscripts

Localized rest and stress human cardiac creatine kinase reaction kinetics at 3 tesla

William T Clarke^{1,2*}, Mark A Peterzan¹, Jennifer J Rayner¹, Rana A Sayeed³, Mario Petrou³, George Krasopoulos³, Hannah A Lake⁴, Betty Raman¹, William D Watson¹, Pete Cox⁵, Moritz J Hundertmark¹, Andrew P Apps¹, Craig A Lygate⁴, Stefan Neubauer¹, Oliver J Rider^{1**} and Christopher T Rodgers^{1,6**}

¹ Oxford Centre for Clinical Magnetic Resonance Research (OCMR), Division of Cardiovascular Medicine RDM, University of Oxford, Level 0, John Radcliffe Hospital, Oxford, OX3 9DU, UK.

² Wellcome Centre for Integrative Neuroimaging, FMRIB, University of Oxford, John Radcliffe Hospital, Oxford, OX3 9DU, UK.

³ Department of Cardiothoracic Surgery, John Radcliffe Hospital, Oxford University Hospitals NHS Foundation Trust, Oxford, OX3 9DU, UK.

⁴ Department of Cardiovascular Medicine, University of Oxford, Wellcome Trust Centre for Human Genetics, Roosevelt Drive, Oxford OX3 7BN, UK

⁵ Department of Physiology Anatomy, University of Oxford, Parks Road, Sherrington Building, Oxford OX1 3PT, UK.

⁶ Wolfson Brain Imaging Centre, University of Cambridge, Box 65, Cambridge Biomedical Campus, Cambridge, CB2 0QQ, UK.

* To whom correspondence should be addressed, ** Joint Senior Authors

Running Heading: Stress human myocardial CK kinetics at 3T

Word count: 4600

Figure and table count: 6 figures, 3 tables: total 9.

Proofs to be sent to:

William T. Clarke
Wellcome Centre for Integrative Neuroimaging, FMRIB
Level 0
John Radcliffe Hospital
Oxford
OX3 9DU.
UK.

william.clarke@ndcn.ox.ac.uk

Tel: 01865 610475

Abstract

Purpose

Changes in the kinetics of the creatine kinase (CK) shuttle are sensitive markers of cardiac energetics but are typically measured at rest and in the prone position. This study aims to measure CK kinetics during pharmacological stress at 3T, with measurement in the supine position. A shorter “stressed saturation transfer” (StreST) extension to the triple repetition time saturation transfer (TRiST) method is proposed. We assess scanning in a supine position and validate the MR measurement against biopsy assay of CK activity. We report normal ranges of stress CK forward rate (k_f^{CK}) for healthy volunteers and obese patients.

Theory and Methods

TRiST measures k_f^{CK} in 40 minutes at 3T. StreST extends the previously developed TRiST to also make a further k_f^{CK} measurement during <20min of dobutamine stress. We test our TRiST implementation in skeletal muscle and myocardium in both prone and supine positions. We evaluate StreST in the myocardium of six healthy volunteers and 34 obese subjects. We validated MR-measured k_f^{CK} against biopsy assays of CK activity.

Results

TRiST k_f^{CK} values matched literature values in skeletal muscle ($k_f^{CK} = 0.25 \pm 0.03 \text{ s}^{-1}$ vs $0.27 \pm 0.03 \text{ s}^{-1}$) and myocardium when measured in the prone position ($0.32 \pm 0.15 \text{ s}^{-1}$), but a significant difference was found for TRiST k_f^{CK} measured supine ($0.24 \pm 0.12 \text{ s}^{-1}$). This difference was due to different respiratory- and cardiac-motion-induced B_0 changes in the two positions. Using supine TRiST, cardiac k_f^{CK} values for normal-weight subjects were $0.15 \pm 0.09 \text{ s}^{-1}$ at rest and $0.17 \pm 0.15 \text{ s}^{-1}$ during stress. For obese subjects k_f^{CK} was $0.16 \pm 0.07 \text{ s}^{-1}$ at rest and $0.17 \pm 0.10 \text{ s}^{-1}$ during stress. Rest myocardial k_f^{CK} and CK activity from LV biopsies of the same subjects correlated ($R=0.43$, $p=0.03$).

Conclusion

We present an independent implementation of TRiST on the Siemens platform using a commercially available coil. Our extended StreST protocol enables cardiac k_f^{CK} to be measured during dobutamine-induced stress in the supine position.

Keywords

³¹P magnetic resonance spectroscopy, cardiac, creatine kinase, energy metabolism, high-energy phosphate, phosphorus, saturation transfer, TRiST, StreST.

Abbreviations

AHP - adiabatic half-passage (pulse)
ATP - adenosine triphosphate
BMI - body-mass-index
CK - creatine kinase
CSI - chemical shift imaging
DANTE - delay alternating with nutation for tailored excitation
ECG - electrocardiogram
FAST - four-angle saturation transfer
 k_f^{CK} - pseudo first-order forward rate
LV - left ventricular
PCr - phosphocreatine
StreST - stress saturation-transfer
TRiST - triple repetition time saturation transfer
TwIST - Two repetition time saturation transfer

Introduction

The rate and flux of the creatine kinase (CK) exchange mechanism have been shown to be sensitive measures of heart failure(1), which is a prevalent and burdensome disease (2,3).

The rate can be characterised by the pseudo first-order forward rate constant, k_f^{CK} .

Phosphorus magnetic resonance spectroscopy (^{31}P -MRS) enables non-invasive measurement of myocardial k_f^{CK} (4). In addition to measuring k_f^{CK} in myocardium at rest, measuring k_f^{CK} during pharmacologically-induced stress would enable us to understand the effect of a perturbed CK mechanism in the stressed human heart (1,5).

Schär et al introduced the triple repetition time saturation transfer (TRiST) sequence to measure CK kinetics by ^{31}P -MRS at 3T (6). A TRiST acquisition lasts 40 min (out of complete protocol totalling 84 min); it measures k_f^{CK} in a one-dimensional coronal stack of slices covering the heart and chest wall (7). 1D-localised k_f^{CK} measurement during inotropic stress was achieved by Weiss et al at 1.5 T using the four-angle saturation transfer (FAST) and the derived "FASTest" method (1,4). However, FAST and FASTest rely on small-angle adiabatic pulses, which are not achievable at 3T due to radiofrequency power requirements, power deposition and T_2 relaxation (8). The 3T TRiST protocol offers an established measurement technique which can be included in a larger cardiac ^1H MR protocol on the same scanner. Whilst 7T ^{31}P -MRS has been used for 3D-localised k_f^{CK} measurements, the existing published methods have long duration and the higher field strength restricts the recruitment of subjects who have undergone surgical procedures (9).

An increase in myocardial work can be reliably maintained, without physical exercise (and therefore motion), by administering dobutamine intravenously. However, the duration of intravenous infusion should be kept to a minimum length. Current guidelines prescribe 15 minute stress protocols(10) and they recommend patients should be scanned in the supine position, for safety in case of arrhythmia. Measuring k_f^{CK} within this timeframe is currently only possible using the "Two repetition time saturation transfer" (TwIST) method, published during the course of this study (7). However, although TwIST assumes a fixed phosphocreatine (PCr) intrinsic longitudinal relaxation time (T_1^*) i.e. in the hypothetical case of PCr not undergoing chemical exchange, it is not yet known whether T_1^* remains constant in clinically-relevant groups; e.g. obese, normal-weight, and heart failure.

We therefore propose to perform stress k_f^{CK} measurements at 3T in two steps: first, derive a per-subject baseline PCr T_1^* with TRiST; and second, performing two further scans during dobutamine-induced stress to record the stress k_f^{CK} in less than 20 minutes of dobutamine infusion. This stress saturation-transfer (StreST) protocol yields a stack of 1D-localised k_f^{CK} measurements at rest *and stress*. We describe below the implementation of StreST and validate the underlying TRiST method in skeletal muscle, in human myocardium in the prone position and subsequently in the supine position, where we correlate surgical left ventricular (LV) biopsy-obtained CK activity against pre-operative myocardial k_f^{CK} in a set of within-patient paired measurements. We then demonstrate StreST by using it to record normative ranges of rest *and stress* k_f^{CK} in the myocardium of normal volunteers and in older obese and age-matched control cohorts.

Theory

CK regenerates adenosine triphosphate (ATP) from PCr according to the equilibrium expression $\text{PCr}^{2-} + \text{MgADP}^- + \text{H}^+ \rightleftharpoons \text{Cr} + \text{MgATP}^{2-}$. CK provides the temporal energy reserve in muscle. TRiST uses steady-state saturation of the terminal (γ) phosphate-group of ATP to measure k_f^{CK} , the pseudo first-order rate constant of the CK reaction in the forward (ATP-generating) direction. Since the ^{31}P nuclei in PCr and γ -ATP are undergoing two-site exchange, continuous saturation of γ -ATP allows the forward exchange rate constant to be determined using

$$k_f^{\text{CK}} = \frac{1}{T_1'} \left(1 - \frac{M'_{\text{PCr}}}{M_{\text{PCr}}^{\text{Ctrl}}} \right). \quad [2]$$

Table 1 summarises each parameter's physical meaning. TRiST measures T_1' , M'_{PCr} and $M_{\text{PCr}}^{\text{Ctrl}}$. This requires three steps: two to measure M'_{PCr} and T_1' using the dual-TR method(8), and a third to measure $M_{\text{PCr}}^{\text{Ctrl}}$ (see Figure 1).

The intrinsic longitudinal relaxation time T_1^* , can be computed from(11)

$$T_1^* = T_1' \frac{M_{\text{PCr}}^{\text{Ctrl}}}{M'_{\text{PCr}}}. \quad [3]$$

Therefore, by substituting Eq. [2], Eq. [1] may be recast in terms of T_1^* rather than T_1' (4):

$$k_f^{\text{CK}} = \frac{1}{T_1^*} \left(\frac{M_{\text{PCr}}^{\text{Ctrl}}}{M'_{\text{PCr}}} - 1 \right). \quad [4]$$

T_1^* is a hypothetical longitudinal relaxation constant for a molecule without chemical exchange. Assuming that T_1^* does not change from one scan to the next (e.g. in myocardium at rest vs under stress), then an additional measurement of k_f^{CK} may be made in two steps: measuring $M_{\text{PCr}}^{\text{Ctrl}}$ and M'_{PCr} . This is a similar assumption to that used in the "FASTer"/"FASTest" adaptation of the FAST method (4).

StreST protocol

Our new "StreST" protocol comprises a rest measurement of k_f^{CK} and PCr T_1^* using TRiST (four steps) and a measurement of k_f^{CK} during intravenous pharmacological stress (two additional steps). The six (4+2) steps are given in Table 2. All steps are completed in a single scanning session.

In future studies using the proposed StreST protocol, subjects will be scanned in the supine position, instead of the prone position used in the original TRiST studies. Prone scanning is considered to be unsafe for a cardiac monitoring perspective, especially when scanning patients with heart failure who may be at greater risk of dangerous arrhythmia. 1/400 patients receiving dobutamine experience a life-threatening arrhythmia (12).

Methods

All subjects were recruited in a manner approved by the local research ethics committee. All participants gave written informed consent.

Hardware, sequence & spectral analysis

All experiments used a 3T TIM Trio MR scanner (Siemens, Erlangen, Germany). The scanner's body coil was used for ^1H localisation. A 10 cm loop transmit-receive surface coil (Pulse Teq, Chobham, UK) tuned to the phosphorus frequency was used for spectroscopy. The ^{31}P coil was matched for each subject using an RF sweeper (Morris Instruments Inc., Ottawa, Canada). Coil loading was measured by inversion-recovery on a phenylphosphonic acid/ethanol/chromium acetylacetonate fiducial fixed at the centre of the coil, as described in reference (13), and expressed as a "reference voltage" (the RMS RF voltage giving a 1 ms

1
2
3
4
5
6
7
8
9
10 180° pulse). The ^{31}P coil was positioned above the apical myocardium of the subject. The
11 positioning was checked using ^1H localiser images of the heard-heart and coil fiducial,
12 repositioning was carried out based on those images.
13

Commented [WC1]: R1.1

14
15 TRIST was implemented on the Siemens platform, following the description in reference (6),
16 as follows. The vendor's 1D chemical shift imaging (CSI) sequence was modified to
17 continuously selectively saturate a chosen frequency whilst waiting to detect an R-wave
18 from an electrocardiogram (ECG) monitor attached to the subject. Once an R-wave was
19 detected saturation was continued for a further "trigger delay" until diastole, at which point
20 an adiabatic half-passage (AHP) excitation pulse, 1D phase encoding gradients and free-
21 induction-decay readout were applied. Diastole was chosen to minimise myocardial motion.
22
23

24
25 The selective saturation was provided by a train of amplitude-modulated delay alternating
26 with nutation for tailored excitation (DANTE) pulses (6). B_1 -insensitive 90° excitation was
27 provided by frequency-cycled AHP pulses (8).
28

29
30 Spectra were analysed, as in reference (6), by measuring the amplitude of the phased and
31 apodized PCr peak relative to the baseline. Raw data from TRIST scans on the 3T Achieva
32 Philips scanner at Johns Hopkins were kindly supplied by Dr Schar and used to validate our
33 fitting approach. k_f^{CK} , T_1' and T_1^* were calculated as described in the theory section (Eq. 1)
34 and reference (6). The amount of direct (or spill-over) saturation of PCr by the DANTE pulse
35 ("Q") was calculated as the ratio of $M_{\text{PCr}}^{\text{ctrl}} / M_{0,\text{PCr}}$. (Q = 1 in the ideal case when there is no
36 direct saturation, but only saturation via chemical exchange from saturated γ -ATP.) Spectra
37 from cardiac slices were selected using the transverse ^1H localiser and analysed on a per-
38 slice basis.
39
40
41
42

43 Literature values

44
45 We surveyed the literature for values of k_f^{CK} in human myocardium and skeletal muscle
46 (Table 3). We used the arithmetic means of the literature k_f^{CK} values and standard deviations
47 for both tissues as a reference to validate our results.
48
49
50
51
52
53
54
55
56
57
58
59
60

Validation of TRiST implementation

Skeletal muscle (calf)

We validated our TRiST implementation in the calf muscle of nine healthy volunteers (8 male, 30.6 ± 3.8 years old, 74.1 ± 11.3 kg). The subjects were positioned feet-first-supine in the scanner with the ^{31}P loop coil under one leg. After ^1H localisation, the 1D-CSI grid was positioned running in the anterior-posterior direction. The protocol followed steps 1-4 in Table 2. Other parameters were: 160 mm field of view (FOV), 16 slices, 3 kHz bandwidth, 512 spectral points, and 200V AHP transmit voltage (corresponding to 800W peak power, and approximately $35 \mu\text{T B}_1^+$ in vivo). Selective saturation of γ -ATP and control saturation were achieved using 35V DANTE pulses (corresponding to 24.5W peak power, and approximately $6 \mu\text{T B}_1^+$ in vivo).

Myocardium in prone position

Ten healthy volunteer subjects (6 male, 29.6 ± 4.9 years old, 70.7 ± 18.2 kg) were scanned using the newly implemented TRiST protocol (steps 1-4, rest k_f^{CK} only) to measure myocardial k_f^{CK} . The scans were completed in the prone position as per previously published methods.

CSI acquisition parameters were as follows: 160mm FOV, 16-step matrix, 3 kHz bandwidth, 512 samples. The CSI grid was positioned perpendicular to a transverse localiser covering the heart, with the CSI delineated dimension aligned coronally (parallel to the band of skeletal muscle lying between the coil and the heart). The AHP transmit voltage was 210 V (i.e. 882W peak power), and the amplitude modulated DANTE voltage was maximised within the constraints of the specific absorption rate (SAR) for the short TR scan (typically to ~ 30 V, i.e. 18W peak power). Spectra from cardiac slices were selected using the transverse ^1H localisers for analysis as described above. The data from the most apical slice containing only myocardium and blood (but not skeletal muscle) were also analysed separately. The coil to slice distance was < 60 mm for these slices.

Myocardium in supine position

As detailed above, as the full StreST protocol will include administering intravenous dobutamine, for which it is preferred to position the subject supine. To test whether the change of position (prone to supine) affects the initial TRiST measurement in the StreST

1
2
3
4
5
6
7
8
9
10 protocol, we scanned the same ten subjects as used in the previous section (6 male,
11 29.6±4.9 years old, 70.7±18.2 kg) again. This time, scans were in the supine position, using
12 the newly implemented TRiST protocol (steps 1-4, rest k_f^{CK} only). Other acquisition and
13 analysis parameters were identical to the previous section.
14
15

16 Effect of intra-scan B_0 fluctuation

17 The potential effects of respiratory and cardiac motion induced B_0 changes on TRiST k_f^{CK}
18 values were analysed using Bloch simulations of the full TRiST protocol. A dual-echo CINE
19 gradient echo sequence was used to measure the range of B_0 values present in the un-
20 shimmed apical myocardium of a single subject in different cardiac phases and respiratory
21 states in both supine and prone positions. A sinusoidal frequency sweep with amplitude of
22 0, 20, 40, 60 and 80 Hz was applied to the Bloch simulation to simulate respiratory motion.
23 The AHP pulse was simulated with three different B_1 magnitudes: 12, 23 and 35 μT , and the
24 DANTE saturation pulse was scaled appropriately to simulate the experiment. Simulations
25 were run with 10000 repetitions, each having a random initial cardiac and respiratory phase.
26 Each independent step of TRiST was simulated and combined to give a measured k_f^{CK} .
27 Simulation parameters were taken from Table 1 (Heart muscle) in Reference (14), with k_f^{CK}
28 varied from 0.1 to 0.5 s^{-1} . SNR was calculated for PCr and $\gamma\text{-ATP}$, the simulation was scaled
29 so the PCR SNR in step 4 was equal to 15.
30
31
32
33
34
35

36 Validation of MRS measured k_f^{CK} by surgical biopsy

37 In a cohort of 25 subjects listed for clinically indicated surgery for either severe aortic
38 stenosis with preserved ($n = 18$) or impaired ($n = 4$) left ventricular ejection fraction (LVEF \geq
39 or $< 55\%$ respectively), severe primary mitral regurgitation ($n = 2$), or atrial myxoma ($n = 1$),
40 k_f^{CK} was measured by supine TRiST and compared to CK activity measured ex-vivo from
41 surgical LV biopsies.
42
43
44

45 All subjects pre-operatively underwent the TRiST MRS protocol in the supine position as
46 described in the previous section. k_f^{CK} was measured for the most apical voxel identified as
47 purely myocardium on ^1H localisers. Intra-operative biopsies from LV septal endocardium
48 were obtained by the operator 10-15 minutes after cardiopulmonary bypass was
49 established, then immediately placed into liquid nitrogen and stored at -80°C .
50
51
52
53
54
55
56
57
58
59
60

1
2
3
4
5
6
7
8
9
10 For the measurement of CK activity a heaped spatula-full of frozen, crushed LV tissue was
11 combined with CK-NAC reagent (Thermo Fisher Scientific catalogue code TR14010) and the
12 prescribed series of reactions were monitored using a spectrophotometer to measure the
13 absorbance of NADH at 340nm and 37 °C over three minutes (15-17). CK activity (IU/mL)
14 was calculated from the rate of change in absorbance of NADH, corrected for reaction
15 volume and an assay-specific correction factor, averaged over three runs and normalised to
16 Lowry protein (mg/mL). Results are presented as CK activity (IU/mg protein). MRS measured
17 CK rate constant was then correlated with biopsy-measured CK activity.
18
19
20
21

22 Validation of the stress k_f^{CK} measurement (StreST) in healthy volunteers

23 The validity of the final reduced-time k_f^{CK} measurement (from steps 5 and 6 in the full
24 StreST protocol) was tested in six healthy volunteers (male, 31±9 years, 75±8 kg). After the
25 initial TRiST measurement (steps 1-4), the follow-on measurement (steps 5&6) was made
26 without repositioning and with the subject still at rest (i.e. a “null stress” control condition).
27 The PCr matched-filtered signal-to-noise ratio (SNR) of the control acquisition (step 4 in
28 Table 2) was determined. The k_f^{CK} , T_1' , T_1^* and Q were reported.
29
30
31
32

33 Reproducibility of the PCr amplitude of individual scans was assessed from the 4th and 5th
34 scans, which are acquired with identical protocols in this validation step (i.e. corresponding
35 to rest and dobutamine-stress scans in patients). Two methods of measuring M_{PCr}' were
36 compared: (i) by saturation-correction in TRiST; and (ii) directly from the 6th StreST step (see
37 Table 2). The correlation and Bland-Altman statistics for these two k_f^{CK} measurements were
38 computed.
39
40
41
42

43 StreST in obese subjects and age-matched controls

44 As many cardiac patients are obese, to allow the measurement to be validated in a real-
45 world population, the full StreST protocol (steps 1-6), including dobutamine-induced stress
46 during the second measurement was performed in age-matched obese and normal-weight
47 volunteers. StreST data were acquired from an obese cohort (N=18, 5 male, 13 female, aged
48 49±13 years, with body-mass-index (BMI) of 35±5), and a normal-weight control cohort
49 (N=6, 1 male, 5 female, aged 53±22 years, with BMI of 24 ± 2). TRiST alone (steps 1-4) was
50 run in ten further normal-weight volunteers (7 male, 3 female, 40±21 years, BMI 23±3).
51
52
53
54
55
56
57
58
59
60

1
2
3
4
5
6
7
8
9
10 For stress scans, dobutamine was administered intravenously, starting at $5 \mu\text{g kg}^{-1} \text{min}^{-1}$, and
11 increasing the infusion rate every 3 minutes until a target heart rate of 65% maximum heart
12 rate (i.e. $220 - \text{age in years}$) was achieved; this target heart rate was then maintained at a
13 steady state for ~ 18 minutes whilst the additional StreST measurements (steps 5-6) were
14 made. Spectra from cardiac slices were selected using the transverse ^1H localisers for
15 analysis as described above. The data from the most apical slice containing only
16 myocardium and blood (but not skeletal muscle) were also analysed separately. The coil to
17 slice distance was < 60 mm for these slices.
18
19
20
21

22 Results

23 Literature values

24 The results of the survey of literature k_r^{CK} are contained in Table 3. The inter-study mean \pm
25 SD k_r^{CK} values were $0.27 \pm 0.04 \text{ s}^{-1}$ (skeletal muscle) and $0.32 \pm 0.07 \text{ s}^{-1}$ (myocardium).
26
27
28
29

30 Validation of TRiST implementation

31 Skeletal muscle (calf)

32 In all subjects, seven or more slices were identified in the transverse ^1H localiser images as
33 containing mainly skeletal muscle. The mean (\pm SD) PCr SNR in the control saturation
34 acquisition (step 4) was 45 ± 32 . Example spectra are shown in Figure 2a.
35
36

37 Consistent T_1' and k_r^{CK} values were found across the 5 slices corresponding to 20 – 60 mm
38 from the coil in all subjects. The average T_1' in these slices was $2.2 \pm 0.4 \text{ s}$, and k_r^{CK} was
39 $0.25 \pm 0.03 \text{ s}^{-1}$. In the two slices furthest from the coil (approx. 70-80 mm), which also
40 contained the tibia and the highest amount of subcutaneous fat, T_1' was higher and k_r^{CK}
41 lower (Figure 2 b&e). T_1' was less consistent across slices and between the subjects (Figure
42 2c).
43
44
45
46

47 Complete saturation ($>95\%$ saturation) of γ -ATP was observed in all subjects, in all slices
48 except the 2 furthest from the coil; in these slices the residual γ -ATP level was $12 \pm 3\%$ of the
49 control saturation scan. The ratio of the control-saturation PCr peak to the no-saturation
50 PCr peak ("Q", a measure of direct saturation of PCr by DANTE) was >0.5 for depths from
51
52
53
54
55
56
57
58
59
60

1
2
3
4
5
6
7
8
9
10 30–80 mm (Figure 2d). In the closest slices to the coil (10 & 20 mm) Q was <0.5, i.e.
11 substantial direct saturation occurred.

12
13 Results from this subsection and others in “results” are summarised in Supporting Table 1.

14 15 **Myocardium in prone position**

16 From the ten healthy volunteers scanned in the prone position, 29 slices were identified as
17 corresponding to myocardium in the transverse ^1H localisers and had sufficient SNR for
18 analysis (PCr SNR > 10 in the control scan).

19
20
21 The all-slice mean \pm SD k_f^{CK} was $0.29 \pm 0.09 \text{ s}^{-1}$. Analysing only the most anterior purely
22 myocardial slice in each subject (10 slices) gave mean k_f^{CK} of $0.32 \pm 0.15 \text{ s}^{-1}$.

23
24
25 The all-slice mean T_1' was $2.7 \pm 1.0 \text{ s}$ and T_1^* was $4.7 \pm 1.6 \text{ s}$. The mean (\pm SD) PCr SNR was $18 \pm$
26 8 . Analysing only the most anterior purely myocardial slice in each subject gave SNR = $19 \pm$
27 5 , $T_1' = 2.9 \pm 0.6 \text{ s}$, and $T_1^* = 5.2 \pm 0.8 \text{ s}$.

28 29 **Myocardium in supine position**

30 The same ten healthy volunteers were also scanned in the supine position. In this dataset,
31 30 slices were identified as corresponding to myocardium in the transverse ^1H localisers and
32 had sufficient SNR for analysis.

33
34
35 The all-slice mean \pm SD k_f^{CK} was $0.15 \pm 0.10 \text{ s}^{-1}$. Analysing only the most anterior purely
36 myocardial slice in each subject gave a mean k_f^{CK} of $0.24 \pm 0.12 \text{ s}^{-1}$.

37
38
39 The all-slice T_1' was $2.5 \pm 1.1 \text{ s}$, and T_1^* was $4.4 \pm 1.9 \text{ s}$. The mean (\pm SD) PCr SNR was 16 ± 9 .
40 Analysing only the most anterior purely myocardial slice in each subject gave SNR = 17 ± 6 ,
41 $T_1' = 2.3 \pm 0.5 \text{ s}$, and $T_1^* = 4.6 \pm 1.0 \text{ s}$.

42 43 **Effect of intra-scan B_0 fluctuation**

44 The single subject measurement of B_0 established that the mean range of γB_0 experienced in
45 the apical myocardium due to cardiac motion in a ^{31}P experiment is 34.3 Hz (supine) and
46 34.6 Hz (prone), and due to respiratory motion is 66.7 Hz (supine) and 36.1 Hz (prone).
47 (Supporting Figure 1 & 2). As the range of B_0 variation was increased in the simulations the
48 amount of time during the DANTE saturation pulse when $M_{z,\gamma\text{-ATP}} = 0$ decreased (i.e. $\gamma\text{-ATP}$
49 saturation was not achieved at all times), even though the SNR of the residual $\gamma\text{-ATP}$ peak in
50 TRIST steps 2&3 remained very low: SNR < 2.5 (Figure 3 a&b). With increasing B_0 fluctuation
51
52
53
54
55
56
57
58
59
60

1
2
3
4
5
6
7
8
9
10 amplitude and decreasing γ -ATP saturation, the measured k_f^{CK} also decreased (Figure 3c). At
11 the level of the estimated B_0 variation due to respiration in our study, the measured k_f^{CK} was
12 simulated to be 0.61 times the true k_f^{CK} in a supine position and 0.85 times the true k_f^{CK} in
13 the prone position. The linearity of the ratio of measured k_f^{CK} / true k_f^{CK} decreases with
14 increasing B_0 variation (Figure 3d).

17 Validation of MRS measured k_f^{CK} by surgical biopsy

18 From the twenty-five subjects listed for clinically indicated surgery mean (\pm SD) k_f^{CK} was
19 $0.21 \pm 0.10 \text{ s}^{-1}$ and mean (\pm SD) biopsy-measured CK activity was $3.96 \pm 1.70 \text{ IU mg}^{-1} \text{ protein}$.
20 The Pearson's Linear Correlation Coefficient (Pearson's R) was 0.43 with a statistically
21 significant correlation ($p = 0.03$).

22 Validation of the stress k_f^{CK} measurement (StreST) in healthy volunteers

23 All the per-subject and mean k_f^{CK} values from the myocardial and skeletal muscle voxels of
24 the six healthy volunteer rest-rest ("null stress" control) StreST scans are plotted in Figure 4.
25 In these scans 36 slices were identified as corresponding to myocardium in the transverse ^1H
26 localisers and had sufficient SNR for analysis (PCr SNR > 10 in the control scan). The all-slice
27 mean (\pm SD) PCr SNR was 16 ± 9 , T_1' was $2.9 \pm 1.0 \text{ s}$, and T_1^* was $4.8 \pm 1.8 \text{ s}$. The all-slice mean
28 k_f^{CK} of the first measurement (TRIST) was $0.14 \pm 0.08 \text{ s}^{-1}$ and the all-slice mean of the second
29 measurement (dobutamine not administered for this validation experiment) was 0.22 ± 0.14
30 s^{-1} . A per-slice comparison of these k_f^{CK} measurements yielded a correlation of 0.51 (Figure
31 5a). Bland-Altman (Figure 5b) analysis yielded a bias of -0.08 s^{-1} with 95% confidence
32 intervals (CIs) of $+0.16 \text{ s}^{-1}$ and -0.31 s^{-1} . A paired Student's t-test showed statistical
33 significance between the two measurements ($p = 0.0006$).

34 Analysing only the most anterior purely myocardial slice in each subject (6 slices) gave SNR =
35 15 ± 5 , PCr $T_1' = 3.0 \pm 0.6 \text{ s}$, PCr $T_1^* = 5.7 \pm 0.9 \text{ s}$, k_f^{CK} (first) = $0.18 \pm 0.08 \text{ s}^{-1}$, k_f^{CK} (second) =
36 $0.18 \pm 0.05 \text{ s}^{-1}$, and a per-slice correlation of 0.62. The mean coil-to-voxel distance for these
37 slices was $53 \pm 7 \text{ mm}$. Bland-Altman (Figure 5b) analysis yielded a bias of -0.04 s^{-1} with 95%
38 CIs of $+0.04 \text{ s}^{-1}$ and -0.12 s^{-1} . A paired Student's t-test showed no statistical significance
39 between the two measurements ($p = 0.11$).

40 Further reproducibility measurements are presented in the supporting information. The
41 comparison of the PCr amplitudes of the 4th and 5th steps yielded a correlation of 0.99

(Supporting Figure 3a&b). The comparison of the two methods of calculating M_0' yielded a correlation of 0.96 (Supporting Figure 3c&d).

The coil reference voltage, measuring the degree of coil loading, varied by <10 % for all six subjects, and was within 25% of the values measured in the skeletal muscle validation.

StreST in obese subjects and age-matched controls

In both obese and normal-weight volunteers (34 total) the average k_f^{CK} in all myocardial slices (with PCr SNR > 10) was $0.12 \pm 0.08 \text{ s}^{-1}$. The average PCr SNR was 14 ± 9 across the 209 slices analysed.

Analysing only the most anterior myocardial slice of each subject (34 slices), k_f^{CK} was $0.16 \pm 0.08 \text{ s}^{-1}$ (Figure 6a). The average PCr SNR was 15 ± 6 .

In the subjects that underwent both rest & stress measurements the mean k_f^{CK} at rest was $0.16 \pm 0.07 \text{ s}^{-1}$ (obese) and $0.15 \pm 0.09 \text{ s}^{-1}$ (normal weight). Under stress the values were $0.17 \pm 0.11 \text{ s}^{-1}$ (obese) and $0.17 \pm 0.15 \text{ s}^{-1}$ (normal weight). This data is shown in Figure 6b.

The T_1^* of the two cohorts was $5.69 \pm 1.43 \text{ s}$ for obese and $4.67 \pm 1.92 \text{ s}$ for normal weight subjects (Figure 6c); this difference is statistically significantly (Student's t-test, $p = 0.02$).

Discussion

We have implemented a new StreST protocol for measuring human CK rate constants in the human heart during dobutamine-induced stress. In so doing, we have also implemented the published TRiST protocol measuring k_f^{CK} at rest for the first time on a Siemens scanner, and using a commercially available coil. We have tested StreST (and hence also TRiST) in calf and cardiac muscle and applied it in the hearts of normal volunteers and obese subjects. We have demonstrated a correlation between our MRS measured value of k_f^{CK} and CK activity in human LV biopsies.

Measurements in calf muscle show that our implementation of TRiST measures k_f^{CK} in line with literature values up to 70 mm from coil. The coil loading changed by up to 25% between skeletal muscle and the thorax. Therefore, we expected accurate myocardial measurement in cardiac slices $\leq 70 \text{ mm}$ from the coil, i.e. we expected that k_f^{CK} in apical cardiac slices could be measured robustly. This is corroborated by a Monte Carlo

1
2
3
4
5
6
7
8
9
10 propagation of error analysis (Supporting Figure 4) which suggests the precision and
11 accuracy of the technique is acceptable for PCr SNR > 10. Only apical myocardial slices
12 achieve this SNR level consistently in all subjects. The working depth of the TRiST protocol
13 could be improved by a different choice of coil: e.g. a different design of transmit coil (e.g. a
14 larger loop or two loops in quadrature) would ensure effective saturation and excitation at
15 greater depths. A receive array might also be used for signal reception to improve SNR,
16 although this might come at the expense of greatly increased signal contamination by non-
17 myocardial tissue because spatial localisation in TRiST is reliant on a restricted sensitivity
18 profile of the coil in two dimensions.
19

20
21
22
23 Myocardial k_f^{CK} measured in the prone position further validated the new implementation
24 of TRiST with all cardiac slices in ten subjects giving $0.29 \pm 0.09 \text{ s}^{-1}$ and k_f^{CK} from only the most
25 apical voxel for each subject giving a mean of $0.32 \pm 0.15 \text{ s}^{-1}$, although the standard deviation
26 of this measurement is double that reported in the literature (Table 3). In the supine
27 position, the measured k_f^{CK} throughout this study is much lower than the paired prone
28 estimate, the literature estimate of 0.32 s^{-1} , and our own 7T k_f^{CK} estimate (0.35 ± 0.05) (9). It
29 is therefore likely that the absolute value of k_f^{CK} measured in a supine position is an
30 underestimate. However, simulations of the effect of B_0 variation during respiratory and
31 cardiac cycles and correlation with biopsy measured CK activity in 25 patients indicate that
32 despite the low absolute value of supine MRS measured k_f^{CK} , trends in our measured k_f^{CK}
33 values are still meaningful – i.e. increases or decreases in measured k_f^{CK} correspond to real
34 increases or decreases.
35
36
37
38
39

40 We invested considerable effort in studying the possible causes of the lower supine TRiST
41 k_f^{CK} measurements. A thorough validation of the sequence timings was performed in the
42 vendor simulation environment and by capturing the live waveforms of the triggered
43 sequence using a digital oscilloscope on the scanner. Data shared from Johns Hopkins were
44 used to validate our analysis process, which performed comparably to the Johns Hopkins
45 analysis. Bloch simulations of the TRiST method indicated that if constant steady-state
46 saturation of γ -ATP is not maintained completely throughout the mixing time, the measured
47 k_f^{CK} will underestimate the true k_f^{CK} by a predictable scaling that is approximately linear for
48 modest B_0 fluctuation amplitudes (Supporting Figure 5). Note that this effect can occur even
49 when the γ -ATP peak is well suppressed in the observed saturated spectra. It is proposed
50
51
52
53
54
55
56
57
58
59
60

1
2
3
4
5
6
7
8
9
10 that this is produced by B_0 shifts, due to respiration or cardiac motion, intermittently
11 shifting the γ -ATP resonance away from the target selective saturation frequency. We have
12 shown that the range of B_0 experienced in the myocardium is raised in this experiment
13 when the subject is supine rather than prone (approx. 60 Hz range versus 30 Hz). The choice
14 of supine scanning was necessitated in this study for subject safety during pharmacological
15 stress and will be required in our institute for further studies using StreST in patients with
16 established cardiac diseases. Scanning supine also helps coil placement and matching.

17
18
19
20 The effect of B_0 shifts due to respiration was found, by simulation, to decrease the
21 measured k_f^{CK} by approximately 1.6 times for supine scans. This factor was found to be
22 constant for all values of k_f^{CK} as long as the B_0 shifts did not exceed a range of 80 Hz. Above
23 this level the effect is non-linear, decreasing the sensitivity of TRiST to changes in k_f^{CK} . Our
24 simulations also suggest that even in the prone position the true value of k_f^{CK} is likely to be
25 underestimated by the TRiST method. At the measured amplitude of B_0 fluctuation the
26 correction remains mostly linear and so relative changes in k_f^{CK} are preserved for both prone
27 and supine scanning.

28
29
30
31
32 StreST reduces the time of the consecutive measurement from 40 min to 20 min by
33 assuming that the subject's T_1^* is constant, which makes it feasible to measure k_f^{CK} during
34 dobutamine infusion at 3T. Previously, Weiss et al. used an adaptation of the "FAST"
35 protocol to measure k_f^{CK} during stress in 13 minutes at 1.5 T (1). The validation of StreST
36 applied without dobutamine showed that the method is able to reliably measure the same
37 k_f^{CK} in a reduced duration in the most apical, high SNR voxels. It is therefore likely that the
38 assumption of static between-scan T_1^* is reasonable. In voxels with low SNR or experiencing
39 high direct saturation (low Q, e.g. skeletal muscle) the reduced duration measurement does
40 not match the full TRiST measurement and introduces high variance.

41
42
43
44
45 The average PCr T_1^* calculated, as per Eqn. 2, was different for the two cohorts: normal-
46 weight and obese ($p=0.02$). This suggests that to accurately measure stress k_f^{CK} , T_1^* must
47 either be determined per-subject, as in StreST, or per-cohort in a pilot study designed to
48 measure T_1^* . We do not recommend assuming a single PCr T_1^* for all human subjects.

49
50
51 Like TRiST, StreST has diagnostic potential for non-invasively assessing the CK system and by
52 extension a subject's contractile reserve (18). Sensitivity to contractile reserve would be
53
54
55
56
57
58
59
60

1
2
3
4
5
6
7
8
9
10 valuable in patients who are not able to undergo conventional stress testing e.g. severe
11 valvular heart disease. The CK system is also a major mechanism for controlling cytosolic
12 [ADP]. A raised cytosolic [ADP] at stress contributes to increased left ventricular end-
13 diastolic pressure and diastolic dysfunction (19). A raised left ventricular end-diastolic
14 pressure is characteristic of heart failure with preserved ejection fraction, which comprises
15 approximately half of all clinically presenting heart failure cases.
16
17

18
19 Cardiac positron emission tomography (PET) can also measure myocardial metabolic
20 reaction kinetics through the uptake of tracers (20). It is able to confirm viability in
21 suspected hibernating myocardium using glucose tracers (21). PET is able to detect uptake
22 in ingressing inflammatory cells and has emerging roles in detection of prosthetic valve
23 endocarditis (22) and inflammatory atherosclerotic coronary and carotid plaques (23,24).
24 However, the onward metabolism of the tracer after uptake cannot be assessed and it is not
25 possible to distinguish which cell type is responsible using PET alone. The MRS technique
26 presented here is specific to CK expressing cells, i.e. cardiomyocytes. Cardiac MR(S) and PET
27 measure similar information with differing trade-offs in temporal and spatial resolution. The
28 use of both in tandem could offer complementary information (21).
29
30
31
32

33 StreST was demonstrated in a control cohort, as well as an obese cohort. The TRiST
34 component of the protocol was run successfully on 34 out of 35 initial subjects. The full
35 StreST protocol was completed by 17 out of 24 subjects, with five subjects electing not to
36 complete due to discomfort and two scans stopped after exceeding the local limit on
37 maximum scan duration. The mean \pm SD time of a complete StreST protocol was 103 ± 7
38 minutes, Steps 1-6 of StreST take 64 minutes in total. The TRiST and StreST techniques are
39 being applied in ongoing studies, building on the initial cohort scans in this work.
40
41
42
43

44 Conclusion

45
46 In this work, we introduced an extended StreST protocol that enables measurement of k_f^{CK}
47 during a 20-minute dobutamine infusion at 3T. We also independently implemented the
48 TRiST protocol on a Siemens 3T scanner using commercially-available hardware. We
49 compare TRiST measured in the prone and supine position and provide a non-MR validation
50 of MR measured k_f^{CK} . We show by simulations that respiratory-induced motion can lead to
51
52
53
54
55
56
57
58
59
60

1
2
3
4
5
6
7
8
9
10 incomplete γ -ATP saturation during the saturation-transfer phase of the TRiST sequence
11 even in the case where the γ -ATP peak is absent from the saturated spectra. Linear
12 correction can compensate for these effects for light to moderate B_0 -field fluctuation
13 amplitudes.
14
15

16 Acknowledgements

17
18
19 We thank Michael Schar for providing test data to validate our post-processing routines, and
20 Paul Bottomley for discussion of the potential factors that may reduce measured k_f^{CK} .

21
22 Funded by: a Sir Henry Dale Fellowship from the Wellcome Trust and the Royal Society
23 [098436/Z/12/B] to CTR, the BHF Centre of Research Excellence (OJR), a BHF clinical
24 research training fellowship [FS/15/80/31803] to MAP, a BHF fellowship [FS/14/54/30946]
25 to JJR, an NIHR OBRC fellowship to BR, a BHF programme grant [RG/13/8/30266] to CAL and
26 SN, and a DPhil studentship from the Medical Research Council to WTC. We acknowledge
27 support from the Oxford NIHR Biomedical Research Centre.
28

29 References

- 30
31 1. Weiss RG, Gerstenblith G, Bottomley PA. ATP flux through creatine kinase in the normal,
32 stressed, and failing human heart. *P Natl Acad Sci USA* 2005;102(3):808-813.
- 33 2. Mozaffarian D, Benjamin EJ, Go AS, et al. Heart disease and stroke statistics--2015 update: a
34 report from the American Heart Association. *Circulation* 2015;131(4):e29-322.
- 35 3. Townsend N, Williams J, Bhatnagar P, Wickramasinghe K, Rayner M. Cardiovascular disease
36 statistics, 2014. London: British Heart Foundation: 2014.
- 37 4. Bottomley PA, Ouwerkerk R, Lee RF, Weiss RG. Four-angle saturation transfer (FAST) method
38 for measuring creatine kinase reaction rates in vivo. *Magn Reson Med* 2002;47(5):850-863.
- 39 5. Rider OJ, Francis JM, Ali MK, et al. Effects of catecholamine stress on diastolic function and
40 myocardial energetics in obesity. *Circulation* 2012;125(12):1511-1519.
- 41 6. Schar M, El-Sharkawy AMM, Weiss RG, Bottomley PA. Triple Repetition Time Saturation
42 Transfer (TRiST) (31 P Spectroscopy for Measuring Human Creatine Kinase Reaction Kinetics.
43 *Magnetic Resonance in Medicine* 2010;63(6):1493-1501.
- 44 7. Schar M, Gabr RE, El-Sharkawy AM, Steinberg A, Bottomley PA, Weiss RG. Two repetition
45 time saturation transfer (TwIST) with spill-over correction to measure creatine kinase
46 reaction rates in human hearts. *J Cardiovasc Magn R* 2015;17.
- 47 8. El-Sharkawy AM, Schar M, Ouwerkerk R, Weiss RG, Bottomley PA. Quantitative Cardiac P-31
48 Spectroscopy at 3 Tesla Using Adiabatic Pulses. *Magnetic Resonance in Medicine*
49 2009;61(4):785-795.
- 50 9. Clarke WT, Robson MD, Neubauer S, Rodgers CT. Creatine kinase rate constant in the human
51 heart measured with 3D-localization at 7 tesla. *Magn Reson Med* 2017;78(1):20-32.
- 52 10. Becher H, Chambers J, Fox K, et al. BSE procedure guidelines for the clinical application of
53 stress echocardiography, recommendations for performance and interpretation of stress
54 echocardiography: a report of the British Society of Echocardiography Policy Committee.
55 *Heart* 2004;90 Suppl 6:vi23-30.
- 56 11. Spencer RG, Fishbein KW. Measurement of spin-lattice relaxation times and concentrations
57 in systems with chemical exchange using the one-pulse sequence: breakdown of the Ernst
58
59
60

- 1
2
3
4
5
6
7
8
9
10 model for partial saturation in nuclear magnetic resonance spectroscopy. *J Magn Reson* 2000;142(1):120-135.
- 11
12 12. Geleijnse ML, Krenning BJ, Nemes A, et al. Incidence, pathophysiology, and treatment of
13 complications during dobutamine-atropine stress echocardiography. *Circulation*
14 2010;121(15):1756-1767.
- 15 13. Rodgers CT, Clarke WT, Snyder C, Vaughan JT, Neubauer S, Robson MD. Human cardiac 31P
16 magnetic resonance spectroscopy at 7 Tesla. *Magn Reson Med* 2014;72(2):304-315.
- 17 14. Ouwerkerk R, Bottomley PA. On neglecting chemical exchange effects when correcting in
18 vivo (31)P MRS data for partial saturation. *J Magn Reson* 2001;148(2):425-435.
- 19 15. Oliver IT. A spectrophotometric method for the determination of creatine phosphokinase
20 and myokinase. *Biochem J* 1955;61(1):116-122.
- 21 16. Rosalki SB. An improved procedure for serum creatine phosphokinase determination. *J Lab*
22 *Clin Med* 1967;69(4):696-705.
- 23 17. Szasz G, Waldenstrom J, Gruber W. Creatine-Kinase in Serum .6. Inhibition by Endogenous
24 Polyvalent Cations, and Effect of Chelators on the Activity and Stability of Some Assay
25 Components. *Clin Chem* 1979;25(3):446-452.
- 26 18. Tian R, Nascimben L, Kaddurah-Daouk R, Ingwall JS. Depletion of energy reserve via the
27 creatine kinase reaction during the evolution of heart failure in cardiomyopathic hamsters. *J*
28 *Mol Cell Cardiol* 1996;28(4):755-765.
- 29 19. Tian R, Nascimben L, Ingwall JS, Lorell BH. Failure to maintain a low ADP concentration
30 impairs diastolic function in hypertrophied rat hearts. *Circulation* 1997;96(4):1313-1319.
- 31 20. Sarikaya I. Cardiac applications of PET. *Nucl Med Commun* 2015;36(10):971-985.
- 32 21. Kunze KP, Dirschinger RJ, Kossmann H, et al. Quantitative cardiovascular magnetic
33 resonance: extracellular volume, native T1 and 18F-FDG PET/CMR imaging in patients after
34 revascularized myocardial infarction and association with markers of myocardial damage
35 and systemic inflammation. *J Cardiovasc Magn Reson* 2018;20(1):33.
- 36 22. Habib G, Lancellotti P, Antunes MJ, et al. 2015 ESC Guidelines for the management of
37 infective endocarditis: The Task Force for the Management of Infective Endocarditis of the
38 European Society of Cardiology (ESC). Endorsed by: European Association for Cardio-
39 Thoracic Surgery (EACTS), the European Association of Nuclear Medicine (EANM). *Eur Heart J*
40 2015;36(44):3075-3128.
- 41 23. Moss AJ, Adamson PD, Newby DE, Dweck MR. Positron emission tomography imaging of
42 coronary atherosclerosis. *Future Cardiol* 2016;12(4):483-496.
- 43 24. Salata BM, Singh P. Role of Cardiac PET in Clinical Practice. *Curr Treat Options Cardiovasc*
44 *Med* 2017;19(12):93.
- 45 25. Smith CS, Bottomley PA, Schulman SP, Gerstenblith G, Weiss RG. Altered creatine kinase
46 adenosine triphosphate kinetics in failing hypertrophied human myocardium. *Circulation*
47 2006;114(11):1151-1158.
- 48 26. Bottomley PA, Wu KC, Gerstenblith G, Schulman SP, Steinberg A, Weiss RG. Reduced
49 Myocardial Creatine Kinase Flux in Human Myocardial Infarction An In Vivo Phosphorus
50 Magnetic Resonance Spectroscopy Study. *Circulation* 2009;119(14):1918-1924.
- 51 27. Bashir A, Gropler R. Reproducibility of creatine kinase reaction kinetics in human heart: a
52 31P time-dependent saturation transfer spectroscopy study. *NMR in Biomedicine*
53 2014;27(6):663-671.
- 54 28. Valkovic L, Chmelik M, Kukurova IJ, et al. Time-resolved phosphorous magnetization transfer
55 of the human calf muscle at 3 T and 7 T: A feasibility study. *Eur J Radiol* 2013;82(5):745-751.
- 56 29. Parasoglou P, Xia D, Chang G, Convit A, Regatte RR. Three-dimensional mapping of the
57 creatine kinase enzyme reaction rate in muscles of the lower leg. *Nmr in Biomedicine*
58 2013;26(9):1142-1151.
- 59 30. Parasoglou P, Xia D, Chang G, Regatte RR. Three-dimensional Saturation Transfer P-31-MRI
60 in Muscles of the Lower Leg at 3.0 T. *Sci Rep-Uk* 2014;4.

1
2
3
4
5
6
7
8
9
10
11
12
13
14
15
16
17
18
19
20
21
22
23
24
25
26
27
28
29
30
31
32
33
34
35
36
37
38
39
40
41
42
43
44
45
46
47
48
49
50
51
52
53
54
55
56
57
58
59
60

31. Valkovic L, Bogner W, Gajdosik M, et al. One-Dimensional Image-Selected In Vivo Spectroscopy Localized Phosphorus Saturation Transfer at 7T. *Magnetic Resonance in Medicine* 2014;72(6):1509-1515.
32. Buehler T, Kreis R, Boesch C. Comparison of ^{31}P saturation and inversion magnetization transfer in human liver and skeletal muscle using a clinical MR system and surface coils. *Nmr in Biomedicine* 2015;28(2):188-199.
33. Ren JM, Sherry AD, Malloy CR. P-31-MRS of healthy human brain: ATP synthesis, metabolite concentrations, pH, and T-1 relaxation times. *Nmr in Biomedicine* 2015;28(11):1455-1462.

Peer Review Only

Tables

Symbol	Meaning
$M_{0,\text{PCr}}$	Equilibrium longitudinal magnetisation of PCr
$M_{\text{PCr}}^{\text{Ctrl}}$	Measured steady-state longitudinal PCr magnetisation, with mirrored control saturation applied.
$T_{\text{R}}^{\text{Short/Long}}$	Short and long T_{R} , where both $T_{\text{R}}^{\text{Short/Long}} < 5T_1$.
M'_{PCr}	Longitudinal PCr magnetisation, with on-resonance saturation of γ -ATP applied. $T_{\text{R}} \approx 5T_1$
$M'_{\text{PCr}}(T_{\text{R}}^{\text{Short}} / T_{\text{R}}^{\text{Long}})$	Measured steady-state longitudinal PCr magnetisation, with on-resonance saturation of γ -ATP applied.
T_1'	Measured T_1 in the presence of on-resonance saturation of γ -ATP applied.
T_1^*	Intrinsic T_1 , i.e. without the effect of exchange.

Table 1. Meaning of equation variables.

#	θ	T_{R} (s)	Saturation target	Scan averages	Duration (min)	Measured parameters
1	90°	≥ 15	-	2	9	$M_{0,\text{PCr}}, M_{0,\gamma\text{-ATP}}$
2	90°	$2(T_{\text{R}}^{\text{Short}})$	γ -ATP	18	11	$M'_{\text{PCr}}(T_{\text{R}}^{\text{Short}}), [M'_{\gamma\text{-ATP}}(T_{\text{R}}^{\text{Short}})]$
3	90°	$10(T_{\text{R}}^{\text{Long}})$	γ -ATP	8	21	$M'_{\text{PCr}}(T_{\text{R}}^{\text{Long}}), [M'_{\gamma\text{-ATP}}(T_{\text{R}}^{\text{Long}})]$
4	90°	≥ 15	Control	2	9	$M_{\text{PCr}}^{\text{Ctrl}}, M_{\gamma\text{-ATP}}^{\text{Ctrl}}$
5	90°	≥ 15	Control	2	9	$M_{\text{PCr}}^{\text{Ctrl}}, M_{\gamma\text{-ATP}}^{\text{Ctrl}}$
6	90°	≥ 15	γ -ATP	2	9	$M'_{\text{PCr}}, [M'_{\gamma\text{-ATP}}]$

Table 2. Acquisition parameters for the StreST protocol. The first four steps are those of TRiST(6). [...] are parameters required for spill-over correction of k_f^{CK} .

Reference	Method ¹	Localisation ²	Field (T)	N	Study mean \pm SD or range (s ⁻¹)
Myocardium					
(1)	FAST	1D-CSI	1.5	16	0.32 \pm 0.07
(25)	FAST	1D-CSI	1.5	14	0.32 \pm 0.06
(26)	FAST	1D-CSI	1.5	15	0.33 \pm 0.07
(6)	TRiST	1D-CSI	3	8	0.32 \pm 0.07
(7)	TwIST	1D-CSI	3	12	0.33 \pm 0.08
(27)	TDST	1D-ISIS	3	15	0.32 \pm 0.05
<i>average</i>					0.323 \pm 0.067
Skeletal muscle (Calf)					
(6)	TRiST	1D-CSI	3	6	0.26 \pm 0.04
(28)	ST	-	3	6	0.31 \pm 0.04
(28)	ST	-	7	6	0.35 \pm 0.03
(29)	ST	TSE	3	30	0.23-0.29
(30)	Prog. Sat.	TSE	3	23	0.26-0.32
(31)	ST	1D-ISIS	7	23	0.27-0.34
(32)	IT	-	7	10	0.46 \pm 0.09
(33)	IT	-	7	7	0.26 \pm 0.02
<i>average</i>					0.274 \pm 0.041

Table 3. Literature values for human in vivo k_r^{CK} in normal volunteers at rest.

¹ FAST = four-angle saturation transfer, TRiST = triple repetition time saturation transfer, TwIST = two repetition time saturation transfer, TDST = time-dependent saturation transfer, ST = saturation transfer, Prog. Sat. = progressive saturation, IT = inversion transfer, ² CSI = chemical shift imaging, ISIS = image-selected in-vivo spectroscopy, TSE = turbo spin echo.

Localized rest and stress human cardiac creatine kinase reaction kinetics at 3 tesla

William T Clarke^{1,2*}, Mark A Peterzan¹, Jennifer J Rayner¹, Rana A Sayeed³, Mario Petrou³, George Krasopoulos³, Hannah A Lake⁴, Betty Raman¹, William D Watson¹, Pete Cox⁵, Moritz J Hundertmark¹, Andrew P Apps¹, Craig A Lygate⁴, Stefan Neubauer¹, Oliver J Rider^{1**} and Christopher T Rodgers^{1,6**}

¹ Oxford Centre for Clinical Magnetic Resonance Research (OCMR), Division of Cardiovascular Medicine RDM, University of Oxford, Level 0, John Radcliffe Hospital, Oxford, OX3 9DU, UK.

² Wellcome Centre for Integrative Neuroimaging, FMRIB, University of Oxford, John Radcliffe Hospital, Oxford, OX3 9DU, UK.

³ Department of Cardiothoracic Surgery, John Radcliffe Hospital, Oxford University Hospitals NHS Foundation Trust, Oxford, OX3 9DU, UK.

⁴ Department of Cardiovascular Medicine, University of Oxford, Wellcome Trust Centre for Human Genetics, Roosevelt Drive, Oxford OX3 7BN, UK

⁵ Department of Physiology Anatomy, University of Oxford, Parks Road, Sherrington Building, Oxford OX1 3PT, UK.

⁶ Wolfson Brain Imaging Centre, University of Cambridge, Box 65, Cambridge Biomedical Campus, Cambridge, CB2 0QQ, UK.

* To whom correspondence should be addressed, ** Joint Senior Authors

Running Heading: Stress human myocardial CK kinetics at 3T

Word count: 4600

Figure and table count: 6 figures, 3 tables: total 9.

Proofs to be sent to:

William T. Clarke
Wellcome Centre for Integrative Neuroimaging, FMRIB
Level 0
John Radcliffe Hospital
Oxford
OX3 9DU.
UK.

william.clarke@ndcn.ox.ac.uk

Tel: 01865 610475

Abstract

Purpose

Changes in the kinetics of the creatine kinase (CK) shuttle are sensitive markers of cardiac energetics but are typically measured at rest and in the prone position. This study aims to measure CK kinetics during pharmacological stress at 3T, with measurement in the supine position. A shorter “stressed saturation transfer” (StreST) extension to the triple repetition time saturation transfer (TRiST) method is proposed. We assess scanning in a supine position and validate the MR measurement against biopsy assay of CK activity. We report normal ranges of stress CK forward rate (k_f^{CK}) for healthy volunteers and obese patients.

Theory and Methods

TRiST measures k_f^{CK} in 40 minutes at 3T. StreST extends the previously developed TRiST to also make a further k_f^{CK} measurement during <20min of dobutamine stress. We test our TRiST implementation in skeletal muscle and myocardium in both prone and supine positions. We evaluate StreST in the myocardium of six healthy volunteers and 34 obese subjects. We validated MR-measured k_f^{CK} against biopsy assays of CK activity.

Results

TRiST k_f^{CK} values matched literature values in skeletal muscle ($k_f^{\text{CK}} = 0.25 \pm 0.03 \text{ s}^{-1}$ vs $0.27 \pm 0.03 \text{ s}^{-1}$) and myocardium when measured in the prone position ($0.32 \pm 0.15 \text{ s}^{-1}$), but a significant difference was found for TRiST k_f^{CK} measured supine ($0.24 \pm 0.12 \text{ s}^{-1}$). This difference was due to different respiratory- and cardiac-motion-induced B_0 changes in the two positions. Using supine TRiST, cardiac k_f^{CK} values for normal-weight subjects were $0.15 \pm 0.09 \text{ s}^{-1}$ at rest and $0.17 \pm 0.15 \text{ s}^{-1}$ during stress. For obese subjects k_f^{CK} was $0.16 \pm 0.07 \text{ s}^{-1}$ at rest and $0.17 \pm 0.10 \text{ s}^{-1}$ during stress. Rest myocardial k_f^{CK} and CK activity from LV biopsies of the same subjects correlated ($R=0.43$, $p=0.03$).

Conclusion

We present an independent implementation of TRiST on the Siemens platform using a commercially available coil. Our extended StreST protocol enables cardiac k_f^{CK} to be measured during dobutamine-induced stress in the supine position.

Keywords

³¹P magnetic resonance spectroscopy, cardiac, creatine kinase, energy metabolism, high-energy phosphate, phosphorus, saturation transfer, TRiST, StreST.

Abbreviations

AHP - adiabatic half-passage (pulse)
ATP - adenosine triphosphate
BMI - body-mass-index
CK - creatine kinase
CSI - chemical shift imaging
DANTE - delay alternating with nutation for tailored excitation
ECG - electrocardiogram
FAST - four-angle saturation transfer
 k_f^{CK} - pseudo first-order forward rate
LV - left ventricular
PCr - phosphocreatine
StreST - stress saturation-transfer
TRiST - triple repetition time saturation transfer
TwIST - Two repetition time saturation transfer

Introduction

The rate and flux of the creatine kinase (CK) exchange mechanism have been shown to be sensitive measures of heart failure(1), which is a prevalent and burdensome disease (2,3).

The rate can be characterised by the pseudo first-order forward rate constant, k_f^{CK} .

Phosphorus magnetic resonance spectroscopy (^{31}P -MRS) enables non-invasive measurement of myocardial k_f^{CK} (4). In addition to measuring k_f^{CK} in myocardium at rest, measuring k_f^{CK} during pharmacologically-induced stress would enable us to understand the effect of a perturbed CK mechanism in the stressed human heart (1,5).

Schär et al introduced the triple repetition time saturation transfer (TRiST) sequence to measure CK kinetics by ^{31}P -MRS at 3T (6). A TRiST acquisition lasts 40 min (out of complete protocol totalling 84 min); it measures k_f^{CK} in a one-dimensional coronal stack of slices covering the heart and chest wall (7). 1D-localised k_f^{CK} measurement during inotropic stress was achieved by Weiss et al at 1.5 T using the four-angle saturation transfer (FAST) and the derived "FASTest" method (1,4). However, FAST and FASTest rely on small-angle adiabatic pulses, which are not achievable at 3T due to radiofrequency power requirements, power deposition and T_2 relaxation (8). The 3T TRiST protocol offers an established measurement technique which can be included in a larger cardiac ^1H MR protocol on the same scanner. Whilst 7T ^{31}P -MRS has been used for 3D-localised k_f^{CK} measurements, the existing published methods have long duration and the higher field strength restricts the recruitment of subjects who have undergone surgical procedures (9).

An increase in myocardial work can be reliably maintained, without physical exercise (and therefore motion), by administering dobutamine intravenously. However, the duration of intravenous infusion should be kept to a minimum length. Current guidelines prescribe 15 minute stress protocols(10) and they recommend patients should be scanned in the supine position, for safety in case of arrhythmia. Measuring k_f^{CK} within this timeframe is currently only possible using the "Two repetition time saturation transfer" (TwIST) method, published during the course of this study (7). However, although TwIST assumes a fixed phosphocreatine (PCr) intrinsic longitudinal relaxation time (T_{1*}) i.e. in the hypothetical case of PCr not undergoing chemical exchange, it is not yet known whether T_{1*} remains constant in clinically-relevant groups; e.g. obese, normal-weight, and heart failure.

We therefore propose to perform stress k_f^{CK} measurements at 3T in two steps: first, derive a per-subject baseline PCr T_1^* with TRiST; and second, performing two further scans during dobutamine-induced stress to record the stress k_f^{CK} in less than 20 minutes of dobutamine infusion. This stress saturation-transfer (StreST) protocol yields a stack of 1D-localised k_f^{CK} measurements at rest *and stress*. We describe below the implementation of StreST and validate the underlying TRiST method in skeletal muscle, in human myocardium in the prone position and subsequently in the supine position, where we correlate surgical left ventricular (LV) biopsy-obtained CK activity against pre-operative myocardial k_f^{CK} in a set of within-patient paired measurements. We then demonstrate StreST by using it to record normative ranges of rest *and stress* k_f^{CK} in the myocardium of normal volunteers and in older obese and age-matched control cohorts.

Theory

CK regenerates adenosine triphosphate (ATP) from PCr according to the equilibrium expression $PCr^{2-} + MgADP^- + H^+ \rightleftharpoons Cr + MgATP^{2-}$. CK provides the temporal energy reserve in muscle. TRiST uses steady-state saturation of the terminal (γ) phosphate-group of ATP to measure k_f^{CK} , the pseudo first-order rate constant of the CK reaction in the forward (ATP-generating) direction. Since the ^{31}P nuclei in PCr and γ -ATP are undergoing two-site exchange, continuous saturation of γ -ATP allows the forward exchange rate constant to be determined using

$$k_f^{CK} = \frac{1}{T_1'} \left(1 - \frac{M'_{PCr}}{M_{PCr}^{Ctrl}} \right). \quad [2]$$

Table 1 summarises each parameter's physical meaning. TRiST measures T_1' , M'_{PCr} and M_{PCr}^{Ctrl} . This requires three steps: two to measure M'_{PCr} and T_1' using the dual-TR method(8), and a third to measure M_{PCr}^{Ctrl} (see Figure 1).

The intrinsic longitudinal relaxation time T_1^* , can be computed from(11)

$$T_1^* = T_1' \frac{M_{PCr}^{Ctrl}}{M'_{PCr}}. \quad [3]$$

Therefore, by substituting Eq. [2], Eq. [1] may be recast in terms of T_1^* rather than T_1' (4):

$$k_f^{\text{CK}} = \frac{1}{T_1^*} \left(\frac{M_{\text{PCr}}^{\text{Ctrl}}}{M'_{\text{PCr}}} - 1 \right). \quad [4]$$

T_1^* is a hypothetical longitudinal relaxation constant for a molecule without chemical exchange. Assuming that T_1^* does not change from one scan to the next (e.g. in myocardium at rest vs under stress), then an additional measurement of k_f^{CK} may be made in two steps: measuring $M_{\text{PCr}}^{\text{Ctrl}}$ and M'_{PCr} . This is a similar assumption to that used in the “FASTer”/“FASTest” adaptation of the FAST method (4).

StreST protocol

Our new “StreST” protocol comprises a rest measurement of k_f^{CK} and T_1^* using TRiST (four steps) and a measurement of k_f^{CK} during intravenous pharmacological stress (two additional steps). The six (4+2) steps are given in Table 2. All steps are completed in a single scanning session.

In future studies using the proposed StreST protocol, subjects will be scanned in the supine position, instead of the prone position used in the original TRiST studies. Prone scanning is considered to be unsafe for a cardiac monitoring perspective, especially when scanning patients with heart failure who may be at greater risk of dangerous arrhythmia. 1/400 patients receiving dobutamine experience a life-threatening arrhythmia (12).

Methods

All subjects were recruited in a manner approved by the local research ethics committee. All participants gave written informed consent.

Hardware, sequence & spectral analysis

All experiments used a 3T TIM Trio MR scanner (Siemens, Erlangen, Germany). The scanner’s body coil was used for ^1H localisation. A 10 cm loop transmit-receive surface coil (Pulse Teq, Chobham, UK) tuned to the phosphorus frequency was used for spectroscopy. The ^{31}P coil was matched for each subject using an RF sweeper (Morris Instruments Inc., Ottawa, Canada). Coil loading was measured by inversion-recovery on a phenylphosphonic acid/ethanol/chromium acetylacetonate fiducial fixed at the centre of the coil, as described

1
2
3 in reference (13), and expressed as a “reference voltage” (the RMS RF voltage giving a 1 ms
4 180° pulse). The ³¹P coil was positioned above the apical myocardium of the subject. The
5
6 positioning was checked using ¹H localiser images of the heart and coil fiducial, repositioning
7
8 was carried out based on those images.
9

10
11 TRiST was implemented on the Siemens platform, following the description in reference (6),
12
13 as follows. The vendor’s 1D chemical shift imaging (CSI) sequence was modified to
14
15 continuously selectively saturate a chosen frequency whilst waiting to detect an R-wave
16
17 from an electrocardiogram (ECG) monitor attached to the subject. Once an R-wave was
18
19 detected saturation was continued for a further “trigger delay” until diastole, at which point
20
21 an adiabatic half-passage (AHP) excitation pulse, 1D phase encoding gradients and free-
22
23 induction-decay readout were applied. Diastole was chosen to minimise myocardial motion.
24

25 The selective saturation was provided by a train of amplitude-modulated delay alternating
26
27 with nutation for tailored excitation (DANTE) pulses (6). B₁-insensitive 90° excitation was
28
29 provided by frequency-cycled AHP pulses (8).
30

31 Spectra were analysed, as in reference (6), by measuring the amplitude of the phased and
32
33 apodized PCr peak relative to the baseline. Raw data from TRiST scans on the 3T Achieva
34
35 Philips scanner at Johns Hopkins were kindly supplied by Dr Schar and used to validate our
36
37 fitting approach. k_f^{CK} , T_1' and T_1^* were calculated as described in the theory section (Eq. 1)
38
39 and reference (6). The amount of direct (or spill-over) saturation of PCr by the DANTE pulse
40
41 (“Q”) was calculated as the ratio of $M_{PCr}^{Ctrl} / M_{0,PCr}$. (Q = 1 in the ideal case when there is no
42
43 direct saturation, but only saturation via chemical exchange from saturated γ -ATP.) Spectra
44
45 from cardiac slices were selected using the transverse ¹H localiser and analysed on a per-
46
47 slice basis.
48

49 Literature values

50 We surveyed the literature for values of k_f^{CK} in human myocardium and skeletal muscle
51
52 (Table 3). We used the arithmetic means of the literature k_f^{CK} values and standard deviations
53
54 for both tissues as a reference to validate our results.
55
56
57
58
59
60

Validation of TRiST implementation

Skeletal muscle (calf)

We validated our TRiST implementation in the calf muscle of nine healthy volunteers (8 male, 30.6 ± 3.8 years old, 74.1 ± 11.3 kg). The subjects were positioned feet-first-supine in the scanner with the ^{31}P loop coil under one leg. After ^1H localisation, the 1D-CSI grid was positioned running in the anterior-posterior direction. The protocol followed steps 1-4 in Table 2. Other parameters were: 160 mm field of view (FOV), 16 slices, 3 kHz bandwidth, 512 spectral points, and 200V AHP transmit voltage (corresponding to 800W peak power, and approximately $35 \mu\text{T } B_1^+$ in vivo). Selective saturation of $\gamma\text{-ATP}$ and control saturation were achieved using 35V DANTE pulses (corresponding to 24.5W peak power, and approximately $6 \mu\text{T } B_1^+$ in vivo).

Myocardium in prone position

Ten healthy volunteer subjects (6 male, 29.6 ± 4.9 years old, 70.7 ± 18.2 kg) were scanned using the newly implemented TRiST protocol (steps 1-4, rest k_f^{CK} only) to measure myocardial k_f^{CK} . The scans were completed in the prone position as per previously published methods.

CSI acquisition parameters were as follows: 160mm FOV, 16-step matrix, 3 kHz bandwidth, 512 samples. The CSI grid was positioned perpendicular to a transverse localiser covering the heart, with the CSI delineated dimension aligned coronally (parallel to the band of skeletal muscle lying between the coil and the heart). The AHP transmit voltage was 210 V (i.e. 882W peak power), and the amplitude modulated DANTE voltage was maximised within the constraints of the specific absorption rate (SAR) for the short TR scan (typically to ~ 30 V, i.e. 18W peak power). Spectra from cardiac slices were selected using the transverse ^1H localisers for analysis as described above. The data from the most apical slice containing only myocardium and blood (but not skeletal muscle) were also analysed separately. The coil to slice distance was < 60 mm for these slices.

Myocardium in supine position

As detailed above, as the full StreST protocol will include administering intravenous dobutamine, for which it is preferred to position the subject supine. To test whether the change of position (prone to supine) affects the initial TRiST measurement in the StreST

1
2
3 protocol, we scanned the same ten subjects as used in the previous section (6 male,
4 29.6±4.9 years old, 70.7±18.2 kg) again. This time, scans were in the supine position, using
5 the newly implemented TRiST protocol (steps 1-4, rest k_f^{CK} only). Other acquisition and
6 analysis parameters were identical to the previous section.
7
8
9

10 11 Effect of intra-scan B_0 fluctuation

12
13 The potential effects of respiratory and cardiac motion induced B_0 changes on TRiST k_f^{CK}
14 values were analysed using Bloch simulations of the full TRiST protocol. A dual-echo CINE
15 gradient echo sequence was used to measure the range of B_0 values present in the un-
16 shimmed apical myocardium of a single subject in different cardiac phases and respiratory
17 states in both supine and prone positions. A sinusoidal frequency sweep with amplitude of
18 0, 20, 40, 60 and 80 Hz was applied to the Bloch simulation to simulate respiratory motion.
19 The AHP pulse was simulated with three different B_1 magnitudes: 12, 23 and 35 μT , and the
20 DANTE saturation pulse was scaled appropriately to simulate the experiment. Simulations
21 were run with 10000 repetitions, each having a random initial cardiac and respiratory phase.
22 Each independent step of TRiST was simulated and combined to give a measured k_f^{CK} .
23 Simulation parameters were taken from Table 1 (Heart muscle) in Reference (14), with k_f^{CK}
24 varied from 0.1 to 0.5 s^{-1} . SNR was calculated for PCr and $\gamma\text{-ATP}$, the simulation was scaled
25 so the PCR SNR in step 4 was equal to 15.
26
27
28
29
30
31
32
33
34
35
36
37
38

39 Validation of MRS measured k_f^{CK} by surgical biopsy

40 In a cohort of 25 subjects listed for clinically indicated surgery for either severe aortic
41 stenosis with preserved ($n = 18$) or impaired ($n = 4$) left ventricular ejection fraction (LVEF \geq
42 or $< 55\%$ respectively), severe primary mitral regurgitation ($n = 2$), or atrial myxoma ($n = 1$),
43 k_f^{CK} was measured by supine TRiST and compared to CK activity measured ex-vivo from
44 surgical LV biopsies.
45
46
47
48
49

50 All subjects pre-operatively underwent the TRiST MRS protocol in the supine position as
51 described in the previous section. k_f^{CK} was measured for the most apical voxel identified as
52 purely myocardium on ^1H localisers. Intra-operative biopsies from LV septal endocardium
53 were obtained by the operator 10-15 minutes after cardiopulmonary bypass was
54 established, then immediately placed into liquid nitrogen and stored at -80°C .
55
56
57
58
59
60

1
2
3 For the measurement of CK activity a heaped spatula-full of frozen, crushed LV tissue was
4 combined with CK-NAC reagent (Thermo Fisher Scientific catalogue code TR14010) and the
5 prescribed series of reactions were monitored using a spectrophotometer to measure the
6 absorbance of NADH at 340nm and 37 °C over three minutes (15-17). CK activity (IU/mL)
7 was calculated from the rate of change in absorbance of NADH, corrected for reaction
8 volume and an assay-specific correction factor, averaged over three runs and normalised to
9 Lowry protein (mg/mL). Results are presented as CK activity (IU/mg protein). MRS measured
10 CK rate constant was then correlated with biopsy-measured CK activity.
11
12
13
14
15
16
17
18

19 Validation of the stress k_f^{CK} measurement (StreST) in healthy volunteers

20 The validity of the final reduced-time k_f^{CK} measurement (from steps 5 and 6 in the full
21 StreST protocol) was tested in six healthy volunteers (male, 31±9 years, 75±8 kg). After the
22 initial TRiST measurement (steps 1-4), the follow-on measurement (steps 5&6) was made
23 without repositioning and with the subject still at rest (i.e. a “null stress” control condition).
24 The PCr matched-filtered signal-to-noise ratio (SNR) of the control acquisition (step 4 in
25 Table 2) was determined. The k_f^{CK} , T_1' , T_1^* and Q were reported.
26
27
28
29
30
31
32

33 Reproducibility of the PCr amplitude of individual scans was assessed from the 4th and 5th
34 scans, which are acquired with identical protocols in this validation step (i.e. corresponding
35 to rest and dobutamine-stress scans in patients). Two methods of measuring M'_{PCr} were
36 compared: (i) by saturation-correction in TRiST; and (ii) directly from the 6th StreST step (see
37 Table 2). The correlation and Bland-Altman statistics for these two k_f^{CK} measurements were
38 computed.
39
40
41
42
43
44
45

46 StreST in obese subjects and age-matched controls

47 As many cardiac patients are obese, to allow the measurement to be validated in a real-
48 world population, the full StreST protocol (steps 1-6), including dobutamine-induced stress
49 during the second measurement was performed in age-matched obese and normal-weight
50 volunteers. StreST data were acquired from an obese cohort (N=18, 5 male, 13 female, aged
51 49±13 years, with body-mass-index (BMI) of 35±5), and a normal-weight control cohort
52 (N=6, 1 male, 5 female, aged 53±22 years, with BMI of 24 ± 2). TRiST alone (steps 1-4) was
53 run in ten further normal-weight volunteers (7 male, 3 female, 40±21 years, BMI 23±3).
54
55
56
57
58
59
60

1
2
3 For stress scans, dobutamine was administered intravenously, starting at $5 \mu\text{g kg}^{-1} \text{min}^{-1}$, and
4 increasing the infusion rate every 3 minutes until a target heart rate of 65% maximum heart
5 rate (i.e. $220 - \text{age in years}$) was achieved; this target heart rate was then maintained at a
6 steady state for ~ 18 minutes whilst the additional StreST measurements (steps 5-6) were
7 made. Spectra from cardiac slices were selected using the transverse ^1H localisers for
8 analysis as described above. The data from the most apical slice containing only
9 myocardium and blood (but not skeletal muscle) were also analysed separately. The coil to
10 slice distance was < 60 mm for these slices.
11
12
13
14
15
16
17
18

19 Results

20 Literature values

21 The results of the survey of literature k_f^{CK} are contained in Table 3. The inter-study mean \pm
22 SD k_f^{CK} values were $0.27 \pm 0.04 \text{ s}^{-1}$ (skeletal muscle) and $0.32 \pm 0.07 \text{ s}^{-1}$ (myocardium).
23
24
25
26
27
28

29 Validation of TRiST implementation

30 Skeletal muscle (calf)

31 In all subjects, seven or more slices were identified in the transverse ^1H localiser images as
32 containing mainly skeletal muscle. The mean (\pm SD) PCr SNR in the control saturation
33 acquisition (step 4) was 45 ± 32 . Example spectra are shown in Figure 2a.
34
35
36
37
38

39 Consistent T_1' and k_f^{CK} values were found across the 5 slices corresponding to 20 – 60 mm
40 from the coil in all subjects. The average T_1' in these slices was $2.2 \pm 0.4 \text{ s}$, and k_f^{CK} was
41 $0.25 \pm 0.03 \text{ s}^{-1}$. In the two slices furthest from the coil (approx. 70-80 mm), which also
42 contained the tibia and the highest amount of subcutaneous fat, T_1' was higher and k_f^{CK}
43 lower (Figure 2 b&e). T_1^* was less consistent across slices and between the subjects (Figure
44 2c).
45
46
47
48
49
50
51
52

53 Complete saturation ($>95\%$ saturation) of γ -ATP was observed in all subjects, in all slices
54 except the 2 furthest from the coil; in these slices the residual γ -ATP level was $12 \pm 3\%$ of the
55 control saturation scan. The ratio of the control-saturation PCr peak to the no-saturation
56 PCr peak ("Q", a measure of direct saturation of PCr by DANTE) was >0.5 for depths from
57
58
59
60

30–80 mm (Figure 2d). In the closest slices to the coil (10 & 20 mm) Q was <0.5, i.e. substantial direct saturation occurred.

Results from this subsection and others in “results” are summarised in Supporting Table 1.

Myocardium in prone position

From the ten healthy volunteers scanned in the prone position, 29 slices were identified as corresponding to myocardium in the transverse ^1H localisers and had sufficient SNR for analysis (PCr SNR > 10 in the control scan).

The all-slice mean \pm SD k_f^{CK} was $0.29 \pm 0.09 \text{ s}^{-1}$. Analysing only the most anterior purely myocardial slice in each subject (10 slices) gave mean k_f^{CK} of $0.32 \pm 0.15 \text{ s}^{-1}$.

The all-slice mean T_1' was $2.7 \pm 1.0 \text{ s}$ and T_1^* was $4.7 \pm 1.6 \text{ s}$. The mean (\pm SD) PCr SNR was 18 ± 8 . Analysing only the most anterior purely myocardial slice in each subject gave SNR = 19 ± 5 , $T_1' = 2.9 \pm 0.6 \text{ s}$, and $T_1^* = 5.2 \pm 0.8 \text{ s}$.

Myocardium in supine position

The same ten healthy volunteers were also scanned in the supine position. In this dataset, 30 slices were identified as corresponding to myocardium in the transverse ^1H localisers and had sufficient SNR for analysis.

The all-slice mean \pm SD k_f^{CK} was $0.15 \pm 0.10 \text{ s}^{-1}$. Analysing only the most anterior purely myocardial slice in each subject gave a mean k_f^{CK} of $0.24 \pm 0.12 \text{ s}^{-1}$.

The all-slice T_1' was $2.5 \pm 1.1 \text{ s}$, and T_1^* was $4.4 \pm 1.9 \text{ s}$. The mean (\pm SD) PCr SNR was 16 ± 9 . Analysing only the most anterior purely myocardial slice in each subject gave SNR = 17 ± 6 , $T_1' = 2.3 \pm 0.5 \text{ s}$, and $T_1^* = 4.6 \pm 1.0 \text{ s}$.

Effect of intra-scan B_0 fluctuation

The single subject measurement of B_0 established that the mean range of γB_0 experienced in the apical myocardium due to cardiac motion in a ^{31}P experiment is 34.3 Hz (supine) and 34.6 Hz (prone), and due to respiratory motion is 66.7 Hz (supine) and 36.1 Hz (prone). (Supporting Figure 1 & 2). As the range of B_0 variation was increased in the simulations the amount of time during the DANTE saturation pulse when $M_{z,\gamma\text{-ATP}} = 0$ decreased (i.e. $\gamma\text{-ATP}$ saturation was not achieved at all times), even though the SNR of the residual $\gamma\text{-ATP}$ peak in TRiST steps 2&3 remained very low: SNR < 2.5 (Figure 3 a&b). With increasing B_0 fluctuation

1
2
3 amplitude and decreasing γ -ATP saturation, the measured k_f^{CK} also decreased (Figure 3c). At
4 the level of the estimated B_0 variation due to respiration in our study, the measured k_f^{CK} was
5 simulated to be 0.61 times the true k_f^{CK} in a supine position and 0.85 times the true k_f^{CK} in
6 the prone position. The linearity of the ratio of measured k_f^{CK} / true k_f^{CK} decreases with
7 increasing B_0 variation (Figure 3d).
8
9
10
11

12 13 Validation of MRS measured k_f^{CK} by surgical biopsy

14 From the twenty-five subjects listed for clinically indicated surgery mean (\pm SD) k_f^{CK} was
15 0.21 \pm 0.10 s⁻¹ and mean (\pm SD) biopsy-measured CK activity was 3.96 \pm 1.70 IU mg⁻¹ protein.
16 The Pearson's Linear Correlation Coefficient (Pearson's R) was 0.43 with a statistically
17 significant correlation ($p = 0.03$).
18
19
20
21
22

23 Validation of the stress k_f^{CK} measurement (StreST) in healthy volunteers

24 All the per-subject and mean k_f^{CK} values from the myocardial and skeletal muscle voxels of
25 the six healthy volunteer rest-rest ("null stress" control) StreST scans are plotted in Figure 4.
26 In these scans 36 slices were identified as corresponding to myocardium in the transverse ¹H
27 localisers and had sufficient SNR for analysis (PCr SNR > 10 in the control scan). The all-slice
28 mean (\pm SD) PCr SNR was 16 \pm 9, T_1' was 2.9 \pm 1.0 s, and T_1^* was 4.8 \pm 1.8 s. The all-slice mean
29 k_f^{CK} of the first measurement (TRiST) was 0.14 \pm 0.08 s⁻¹ and the all-slice mean of the second
30 measurement (dobutamine not administered for this validation experiment) was 0.22 \pm 0.14
31 s⁻¹. A per-slice comparison of these k_f^{CK} measurements yielded a correlation of 0.51 (Figure
32 5a). Bland-Altman (Figure 5b) analysis yielded a bias of -0.08 s⁻¹ with 95% confidence
33 intervals (CIs) of +0.16 s⁻¹ and -0.31 s⁻¹. A paired Student's t-test showed statistical
34 significance between the two measurements ($p = 0.0006$).
35
36
37
38
39
40
41
42
43
44
45

46 Analysing only the most anterior purely myocardial slice in each subject (6 slices) gave SNR =
47 15 \pm 5, PCr $T_1' = 3.0 \pm 0.6$ s, PCr $T_1^* = 5.7 \pm 0.9$ s, k_f^{CK} (first) = 0.18 \pm 0.08 s⁻¹, k_f^{CK} (second) =
48 0.18 \pm 0.05 s⁻¹, and a per-slice correlation of 0.62. The mean coil-to-voxel distance for these
49 slices was 53 \pm 7 mm. Bland-Altman (Figure 5b) analysis yielded a bias of -0.04 s⁻¹ with 95%
50 CIs of +0.04 s⁻¹ and -0.12 s⁻¹. A paired Student's t-test showed no statistical significance
51 between the two measurements ($p = 0.11$).
52
53
54
55
56

57 Further reproducibility measurements are presented in the supporting information. The
58 comparison of the PCr amplitudes of the 4th and 5th steps yielded a correlation of 0.99
59
60

(Supporting Figure 3a&b). The comparison of the two methods of calculating M_0' yielded a correlation of 0.96 (Supporting Figure 3c&d).

The coil reference voltage, measuring the degree of coil loading, varied by <10 % for all six subjects, and was within 25% of the values measured in the skeletal muscle validation.

StreST in obese subjects and age-matched controls

In both obese and normal-weight volunteers (34 total) the average k_f^{CK} in all myocardial slices (with PCr SNR > 10) was $0.12 \pm 0.08 \text{ s}^{-1}$. The average PCr SNR was 14 ± 9 across the 209 slices analysed.

Analysing only the most anterior myocardial slice of each subject (34 slices), k_f^{CK} was $0.16 \pm 0.08 \text{ s}^{-1}$ (Figure 6a). The average PCr SNR was 15 ± 6 .

In the subjects that underwent both rest & stress measurements the mean k_f^{CK} at rest was $0.16 \pm 0.07 \text{ s}^{-1}$ (obese) and $0.15 \pm 0.09 \text{ s}^{-1}$ (normal weight). Under stress the values were $0.17 \pm 0.11 \text{ s}^{-1}$ (obese) and $0.17 \pm 0.15 \text{ s}^{-1}$ (normal weight). This data is shown in Figure 6b.

The T_1^* of the two cohorts was $5.69 \pm 1.43 \text{ s}$ for obese and $4.67 \pm 1.92 \text{ s}$ for normal weight subjects (Figure 6c); this difference is statistically significantly (Student's t-test, $p = 0.02$).

Discussion

We have implemented a new StreST protocol for measuring human CK rate constants in the human heart during dobutamine-induced stress. In so doing, we have also implemented the published TRiST protocol measuring k_f^{CK} at rest for the first time on a Siemens scanner, and using a commercially available coil. We have tested StreST (and hence also TRiST) in calf and cardiac muscle and applied it in the hearts of normal volunteers and obese subjects. We have demonstrated a correlation between our MRS measured value of k_f^{CK} and CK activity in human LV biopsies.

Measurements in calf muscle show that our implementation of TRiST measures k_f^{CK} in line with literature values up to 70 mm from coil. The coil loading changed by up to 25% between skeletal muscle and the thorax. Therefore, we expected accurate myocardial measurement in cardiac slices $\leq 70 \text{ mm}$ from the coil, i.e. we expected that k_f^{CK} in apical cardiac slices could be measured robustly. This is corroborated by a Monte Carlo

1
2
3 propagation of error analysis (Supporting Figure 4) which suggests the precision and
4 accuracy of the technique is acceptable for PCr SNR > 10. Only apical myocardial slices
5 achieve this SNR level consistently in all subjects. The working depth of the TRiST protocol
6 could be improved by a different choice of coil: e.g. a different design of transmit coil (e.g. a
7 larger loop or two loops in quadrature) would ensure effective saturation and excitation at
8 greater depths. A receive array might also be used for signal reception to improve SNR,
9 although this might come at the expense of greatly increased signal contamination by non-
10 myocardial tissue because spatial localisation in TRiST is reliant on a restricted sensitivity
11 profile of the coil in two dimensions.
12
13
14
15
16
17
18
19

20 Myocardial k_f^{CK} measured in the prone position further validated the new implementation
21 of TRiST with all cardiac slices in ten subjects giving $0.29 \pm 0.09 \text{ s}^{-1}$ and k_f^{CK} from only the most
22 apical voxel for each subject giving a mean of $0.32 \pm 0.15 \text{ s}^{-1}$, although the standard deviation
23 of this measurement is double that reported in the literature (Table 3). In the supine
24 position, the measured k_f^{CK} throughout this study is much lower than the paired prone
25 estimate, the literature estimate of 0.32 s^{-1} , and our own 7T k_f^{CK} estimate (0.35 ± 0.05) (9). It
26 is therefore likely that the absolute value of k_f^{CK} measured in a supine position is an
27 underestimate. However, simulations of the effect of B_0 variation during respiratory and
28 cardiac cycles and correlation with biopsy measured CK activity in 25 patients indicate that
29 despite the low absolute value of supine MRS measured k_f^{CK} , trends in our measured k_f^{CK}
30 values are still meaningful – i.e. increases or decreases in measured k_f^{CK} correspond to real
31 increases or decreases.
32
33
34
35
36
37
38
39
40
41
42

43 We invested considerable effort in studying the possible causes of the lower supine TRiST
44 k_f^{CK} measurements. A thorough validation of the sequence timings was performed in the
45 vendor simulation environment and by capturing the live waveforms of the triggered
46 sequence using a digital oscilloscope on the scanner. Data shared from Johns Hopkins were
47 used to validate our analysis process, which performed comparably to the Johns Hopkins
48 analysis. Bloch simulations of the TRiST method indicated that if constant steady-state
49 saturation of γ -ATP is not maintained completely throughout the mixing time, the measured
50 k_f^{CK} will underestimate the true k_f^{CK} by a predictable scaling that is approximately linear for
51 modest B_0 fluctuation amplitudes (Supporting Figure 5). Note that this effect can occur even
52 when the γ -ATP peak is well suppressed in the observed saturated spectra. It is proposed
53
54
55
56
57
58
59
60

1
2
3 that this is produced by B_0 shifts, due to respiration or cardiac motion, intermittently
4 shifting the γ -ATP resonance away from the target selective saturation frequency. We have
5 shown that the range of B_0 experienced in the myocardium is raised in this experiment
6 when the subject is supine rather than prone (approx. 60 Hz range versus 30 Hz). The choice
7 of supine scanning was necessitated in this study for subject safety during pharmacological
8 stress and will be required in our institute for further studies using StreST in patients with
9 established cardiac diseases. Scanning supine also helps coil placement and matching.

10
11 The effect of B_0 shifts due to respiration was found, by simulation, to decrease the
12 measured k_f^{CK} by approximately 1.6 times for supine scans. This factor was found to be
13 constant for all values of k_f^{CK} as long as the B_0 shifts did not exceed a range of 80 Hz. Above
14 this level the effect is non-linear, decreasing the sensitivity of TRiST to changes in k_f^{CK} . Our
15 simulations also suggest that even in the prone position the true value of k_f^{CK} is likely to be
16 underestimated by the TRiST method. At the measured amplitude of B_0 fluctuation the
17 correction remains mostly linear and so relative changes in k_f^{CK} are preserved for both prone
18 and supine scanning.

19
20 StreST reduces the time of the consecutive measurement from 40 min to 20 min by
21 assuming that the subject's T_1^* is constant, which makes it feasible to measure k_f^{CK} during
22 dobutamine infusion at 3T. Previously, Weiss et al. used an adaptation of the "FAST"
23 protocol to measure k_f^{CK} during stress in 13 minutes at 1.5 T (1). The validation of StreST
24 applied without dobutamine showed that the method is able to reliably measure the same
25 k_f^{CK} in a reduced duration in the most apical, high SNR voxels. It is therefore likely that the
26 assumption of static between-scan T_1^* is reasonable. In voxels with low SNR or experiencing
27 high direct saturation (low Q, e.g. skeletal muscle) the reduced duration measurement does
28 not match the full TRiST measurement and introduces high variance.

29
30 The average PCr T_1^* calculated, as per Eqn. 2, was different for the two cohorts: normal-
31 weight and obese ($p=0.02$). This suggests that to accurately measure stress k_f^{CK} , T_1^* must
32 either be determined per-subject, as in StreST, or per-cohort in a pilot study designed to
33 measure T_1^* . We do not recommend assuming a single PCr T_1^* for all human subjects.

34
35 Like TRiST, StreST has diagnostic potential for non-invasively assessing the CK system and by
36 extension a subject's contractile reserve (18). Sensitivity to contractile reserve would be
37
38
39
40
41
42
43
44
45
46
47
48
49
50
51
52
53
54
55
56
57
58
59
60

1
2
3 valuable in patients who are not able to undergo conventional stress testing e.g. severe
4 valvular heart disease. The CK system is also a major mechanism for controlling cytosolic
5 [ADP]. A raised cytosolic [ADP] at stress contributes to increased left ventricular end-
6
7 [ADP]. A raised cytosolic [ADP] at stress contributes to increased left ventricular end-
8
9 diastolic pressure and diastolic dysfunction (19). A raised left ventricular end-diastolic
10
11 pressure is characteristic of heart failure with preserved ejection fraction, which comprises
12
13 approximately half of all clinically presenting heart failure cases.

14
15 Cardiac positron emission tomography (PET) can also measure myocardial metabolic
16
17 reaction kinetics through the uptake of tracers (20). It is able to confirm viability in
18
19 suspected hibernating myocardium using glucose tracers (21). PET is able to detect uptake
20
21 in ingressing inflammatory cells and has emerging roles in detection of prosthetic valve
22
23 endocarditis (22) and inflammatory atherosclerotic coronary and carotid plaques (23,24).
24
25 However, the onward metabolism of the tracer after uptake cannot be assessed and it is not
26
27 possible to distinguish which cell type is responsible using PET alone. The MRS technique
28
29 presented here is specific to CK expressing cells, i.e. cardiomyocytes. Cardiac MR(S) and PET
30
31 measure similar information with differing trade-offs in temporal and spatial resolution. The
32
33 use of both in tandem could offer complementary information (21).

34
35 StreST was demonstrated in a control cohort, as well as an obese cohort. The TRiST
36
37 component of the protocol was run successfully on 34 out of 35 initial subjects. The full
38
39 StreST protocol was completed by 17 out of 24 subjects, with five subjects electing not to
40
41 complete due to discomfort and two scans stopped after exceeding the local limit on
42
43 maximum scan duration. The mean \pm SD time of a complete StreST protocol was 103 ± 7
44
45 minutes, Steps 1-6 of StreST take 64 minutes in total. The TRiST and StreST techniques are
46
47 being applied in ongoing studies, building on the initial cohort scans in this work.

48 Conclusion

49
50
51 In this work, we introduced an extended StreST protocol that enables measurement of k_f^{CK}
52
53 during a 20-minute dobutamine infusion at 3T. We also independently implemented the
54
55 TRiST protocol on a Siemens 3T scanner using commercially-available hardware. We
56
57 compare TRiST measured in the prone and supine position and provide a non-MR validation
58
59 of MR measured k_f^{CK} . We show by simulations that respiratory-induced motion can lead to
60

1
2
3 incomplete γ -ATP saturation during the saturation-transfer phase of the TRiST sequence
4 even in the case where the γ -ATP peak is absent from the saturated spectra. Linear
5
6 correction can compensate for these effects for light to moderate B_0 -field fluctuation
7
8 amplitudes.
9

10 11 12 Acknowledgements

13
14
15 We thank Michael Schar for providing test data to validate our post-processing routines, and
16 Paul Bottomley for discussion of the potential factors that may reduce measured k_f^{CK} .

17
18 Funded by: a Sir Henry Dale Fellowship from the Wellcome Trust and the Royal Society
19 [098436/Z/12/B] to CTR, the BHF Centre of Research Excellence (OJR), a BHF clinical
20 research training fellowship [FS/15/80/31803] to MAP, a BHF fellowship [FS/14/54/30946]
21 to JJR, an NIHR OBRC fellowship to BR, a BHF programme grant [RG/13/8/30266] to CAL and
22 SN, and a DPhil studentship from the Medical Research Council to WTC. We acknowledge
23 support from the Oxford NIHR Biomedical Research Centre.
24
25
26

27 28 29 References

- 30 1. Weiss RG, Gerstenblith G, Bottomley PA. ATP flux through creatine kinase in the normal,
31 stressed, and failing human heart. *P Natl Acad Sci USA* 2005;102(3):808-813.
- 32 2. Mozaffarian D, Benjamin EJ, Go AS, et al. Heart disease and stroke statistics--2015 update: a
33 report from the American Heart Association. *Circulation* 2015;131(4):e29-322.
- 34 3. Townsend N, Williams J, Bhatnagar P, Wickramasinghe K, Rayner M. Cardiovascular disease
35 statistics, 2014. London: British Heart Foundation: 2014.
- 36 4. Bottomley PA, Ouwerkerk R, Lee RF, Weiss RG. Four-angle saturation transfer (FAST) method
37 for measuring creatine kinase reaction rates in vivo. *Magn Reson Med* 2002;47(5):850-863.
- 38 5. Rider OJ, Francis JM, Ali MK, et al. Effects of catecholamine stress on diastolic function and
39 myocardial energetics in obesity. *Circulation* 2012;125(12):1511-1519.
- 40 6. Schar M, El-Sharkawy AMM, Weiss RG, Bottomley PA. Triple Repetition Time Saturation
41 Transfer (TRiST) (31)P Spectroscopy for Measuring Human Creatine Kinase Reaction Kinetics.
42 *Magnetic Resonance in Medicine* 2010;63(6):1493-1501.
- 43 7. Schar M, Gabr RE, El-Sharkawy AM, Steinberg A, Bottomley PA, Weiss RG. Two repetition
44 time saturation transfer (TwiST) with spill-over correction to measure creatine kinase
45 reaction rates in human hearts. *J Cardiovasc Magn R* 2015;17.
- 46 8. El-Sharkawy AM, Schar M, Ouwerkerk R, Weiss RG, Bottomley PA. Quantitative Cardiac P-31
47 Spectroscopy at 3 Tesla Using Adiabatic Pulses. *Magnetic Resonance in Medicine*
48 2009;61(4):785-795.
- 49 9. Clarke WT, Robson MD, Neubauer S, Rodgers CT. Creatine kinase rate constant in the human
50 heart measured with 3D-localization at 7 tesla. *Magn Reson Med* 2017;78(1):20-32.
- 51 10. Becher H, Chambers J, Fox K, et al. BSE procedure guidelines for the clinical application of
52 stress echocardiography, recommendations for performance and interpretation of stress
53 echocardiography: a report of the British Society of Echocardiography Policy Committee.
54 *Heart* 2004;90 Suppl 6:vi23-30.
- 55 11. Spencer RG, Fishbein KW. Measurement of spin-lattice relaxation times and concentrations
56 in systems with chemical exchange using the one-pulse sequence: breakdown of the Ernst
57
58
59
60

- 1
2
3 model for partial saturation in nuclear magnetic resonance spectroscopy. *J Magn Reson* 2000;142(1):120-135.
- 4
5 12. Geleijnse ML, Krenning BJ, Nemes A, et al. Incidence, pathophysiology, and treatment of
6 complications during dobutamine-atropine stress echocardiography. *Circulation*
7 2010;121(15):1756-1767.
- 8
9 13. Rodgers CT, Clarke WT, Snyder C, Vaughan JT, Neubauer S, Robson MD. Human cardiac 31P
10 magnetic resonance spectroscopy at 7 Tesla. *Magn Reson Med* 2014;72(2):304-315.
- 11
12 14. Ouwerkerk R, Bottomley PA. On neglecting chemical exchange effects when correcting in
13 vivo (31)P MRS data for partial saturation. *J Magn Reson* 2001;148(2):425-435.
- 14
15 15. Oliver IT. A spectrophotometric method for the determination of creatine phosphokinase
16 and myokinase. *Biochem J* 1955;61(1):116-122.
- 17
18 16. Rosalki SB. An improved procedure for serum creatine phosphokinase determination. *J Lab*
19 *Clin Med* 1967;69(4):696-705.
- 20
21 17. Szasz G, Waldenstrom J, Gruber W. Creatine-Kinase in Serum .6. Inhibition by Endogenous
22 Polyvalent Cations, and Effect of Chelators on the Activity and Stability of Some Assay
23 Components. *Clin Chem* 1979;25(3):446-452.
- 24
25 18. Tian R, Nascimben L, Kaddurah-Daouk R, Ingwall JS. Depletion of energy reserve via the
26 creatine kinase reaction during the evolution of heart failure in cardiomyopathic hamsters. *J*
27 *Mol Cell Cardiol* 1996;28(4):755-765.
- 28
29 19. Tian R, Nascimben L, Ingwall JS, Lorell BH. Failure to maintain a low ADP concentration
30 impairs diastolic function in hypertrophied rat hearts. *Circulation* 1997;96(4):1313-1319.
- 31
32 20. Sarikaya I. Cardiac applications of PET. *Nucl Med Commun* 2015;36(10):971-985.
- 33
34 21. Kunze KP, Dirschinger RJ, Kossmann H, et al. Quantitative cardiovascular magnetic
35 resonance: extracellular volume, native T1 and 18F-FDG PET/CMR imaging in patients after
36 revascularized myocardial infarction and association with markers of myocardial damage
37 and systemic inflammation. *J Cardiovasc Magn Reson* 2018;20(1):33.
- 38
39 22. Habib G, Lancellotti P, Antunes MJ, et al. 2015 ESC Guidelines for the management of
40 infective endocarditis: The Task Force for the Management of Infective Endocarditis of the
41 European Society of Cardiology (ESC). Endorsed by: European Association for Cardio-
42 Thoracic Surgery (EACTS), the European Association of Nuclear Medicine (EANM). *Eur Heart J*
43 2015;36(44):3075-3128.
- 44
45 23. Moss AJ, Adamson PD, Newby DE, Dweck MR. Positron emission tomography imaging of
46 coronary atherosclerosis. *Future Cardiol* 2016;12(4):483-496.
- 47
48 24. Salata BM, Singh P. Role of Cardiac PET in Clinical Practice. *Curr Treat Options Cardiovasc*
49 *Med* 2017;19(12):93.
- 50
51 25. Smith CS, Bottomley PA, Schulman SP, Gerstenblith G, Weiss RG. Altered creatine kinase
52 adenosine triphosphate kinetics in failing hypertrophied human myocardium. *Circulation*
53 2006;114(11):1151-1158.
- 54
55 26. Bottomley PA, Wu KC, Gerstenblith G, Schulman SP, Steinberg A, Weiss RG. Reduced
56 Myocardial Creatine Kinase Flux in Human Myocardial Infarction An In Vivo Phosphorus
57 Magnetic Resonance Spectroscopy Study. *Circulation* 2009;119(14):1918-1924.
- 58
59 27. Bashir A, Gropler R. Reproducibility of creatine kinase reaction kinetics in human heart: a
60 31P time-dependent saturation transfer spectroscopy study. *NMR in Biomedicine*
2014;27(6):663-671.
28. Valkovic L, Chmelik M, Kukurova IJ, et al. Time-resolved phosphorous magnetization transfer
of the human calf muscle at 3 T and 7 T: A feasibility study. *Eur J Radiol* 2013;82(5):745-751.
29. Parasoglou P, Xia D, Chang G, Convit A, Regatte RR. Three-dimensional mapping of the
creatine kinase enzyme reaction rate in muscles of the lower leg. *Nmr in Biomedicine*
2013;26(9):1142-1151.
30. Parasoglou P, Xia D, Chang G, Regatte RR. Three-dimensional Saturation Transfer P-31-MRI
in Muscles of the Lower Leg at 3.0 T. *Sci Rep-Uk* 2014;4.

- 1
 - 2
 - 3
 - 4
 - 5
 - 6
 - 7
 - 8
 - 9
 - 10
 - 11
 - 12
 - 13
 - 14
 - 15
 - 16
 - 17
 - 18
 - 19
 - 20
 - 21
 - 22
 - 23
 - 24
 - 25
 - 26
 - 27
 - 28
 - 29
 - 30
 - 31
 - 32
 - 33
 - 34
 - 35
 - 36
 - 37
 - 38
 - 39
 - 40
 - 41
 - 42
 - 43
 - 44
 - 45
 - 46
 - 47
 - 48
 - 49
 - 50
 - 51
 - 52
 - 53
 - 54
 - 55
 - 56
 - 57
 - 58
 - 59
 - 60
31. Valkovic L, Bogner W, Gajdosik M, et al. One-Dimensional Image-Selected In Vivo Spectroscopy Localized Phosphorus Saturation Transfer at 7T. *Magnetic Resonance in Medicine* 2014;72(6):1509-1515.
32. Buehler T, Kreis R, Boesch C. Comparison of ^{31}P saturation and inversion magnetization transfer in human liver and skeletal muscle using a clinical MR system and surface coils. *Nmr in Biomedicine* 2015;28(2):188-199.
33. Ren JM, Sherry AD, Malloy CR. P-31-MRS of healthy human brain: ATP synthesis, metabolite concentrations, pH, and T-1 relaxation times. *Nmr in Biomedicine* 2015;28(11):1455-1462.

Peer Review Only

Tables

Symbol	Meaning
$M_{0,\text{PCr}}$	Equilibrium longitudinal magnetisation of PCr
$M_{\text{PCr}}^{\text{Ctrl}}$	Measured steady-state longitudinal PCr magnetisation, with mirrored control saturation applied.
$T_{\text{R}}^{\text{Short/Long}}$	Short and long T_{R} , where both $T_{\text{R}}^{\text{Short/Long}} < 5T_1$.
M'_{PCr}	Longitudinal PCr magnetisation, with on-resonance saturation of γ -ATP applied. $T_{\text{R}} \approx 5T_1$
$M'_{\text{PCr}}(T_{\text{R}}^{\text{Short}} / T_{\text{R}}^{\text{Long}})$	Measured steady-state longitudinal PCr magnetisation, with on-resonance saturation of γ -ATP applied.
T_1'	Measured T_1 in the presence of on-resonance saturation of γ -ATP applied.
T_1^*	Intrinsic T_1 , i.e. without the effect of exchange.

Table 1. Meaning of equation variables.

#	θ	T_{R} (s)	Saturation target	Scan averages	Duration (min)	Measured parameters
1	90°	≥ 15	-	2	9	$M_{0,\text{PCr}}, M_{0,\gamma\text{-ATP}}$
2	90°	$2(T_{\text{R}}^{\text{Short}})$	γ -ATP	18	11	$M'_{\text{PCr}}(T_{\text{R}}^{\text{Short}}), [M'_{\gamma\text{-ATP}}(T_{\text{R}}^{\text{Short}})]$
3	90°	$10(T_{\text{R}}^{\text{Long}})$	γ -ATP	8	21	$M'_{\text{PCr}}(T_{\text{R}}^{\text{Long}}), [M'_{\gamma\text{-ATP}}(T_{\text{R}}^{\text{Long}})]$
4	90°	≥ 15	Control	2	9	$M_{\text{PCr}}^{\text{Ctrl}}, M_{\gamma\text{-ATP}}^{\text{Ctrl}}$
5	90°	≥ 15	Control	2	9	$M_{\text{PCr}}^{\text{Ctrl}}, M_{\gamma\text{-ATP}}^{\text{Ctrl}}$
6	90°	≥ 15	γ -ATP	2	9	$M'_{\text{PCr}}, [M'_{\gamma\text{-ATP}}]$

Table 2. Acquisition parameters for the StreST protocol. The first four steps are those of TRiST(6). [...] are parameters required for spill-over correction of k_f^{CK} .

Reference	Method ¹	Localisation ²	Field (T)	N	Study mean \pm SD or range (s ⁻¹)
Myocardium					
(1)	FAST	1D-CSI	1.5	16	0.32 \pm 0.07
(25)	FAST	1D-CSI	1.5	14	0.32 \pm 0.06
(26)	FAST	1D-CSI	1.5	15	0.33 \pm 0.07
(6)	TRiST	1D-CSI	3	8	0.32 \pm 0.07
(7)	TwIST	1D-CSI	3	12	0.33 \pm 0.08
(27)	TDST	1D-ISIS	3	15	0.32 \pm 0.05
<i>average</i>					0.323 \pm 0.067
Skeletal muscle (Calf)					
(6)	TRiST	1D-CSI	3	6	0.26 \pm 0.04
(28)	ST	-	3	6	0.31 \pm 0.04
(28)	ST	-	7	6	0.35 \pm 0.03
(29)	ST	TSE	3	30	0.23-0.29
(30)	Prog. Sat.	TSE	3	23	0.26-0.32
(31)	ST	1D-ISIS	7	23	0.27-0.34
(32)	IT	-	7	10	0.46 \pm 0.09
(33)	IT	-	7	7	0.26 \pm 0.02
<i>average</i>					0.274 \pm 0.041

Table 3. Literature values for human in vivo k_r^{CK} in normal volunteers at rest.

¹ FAST = four-angle saturation transfer, TRiST = triple repetition time saturation transfer, TwiST = two repetition time saturation transfer, TDST = time-dependent saturation transfer, ST = saturation transfer, Prog. Sat. = progressive saturation, IT = inversion transfer,
² CSI = chemical shift imaging, ISIS = image-selected in-vivo spectroscopy, TSE = turbo spin echo.

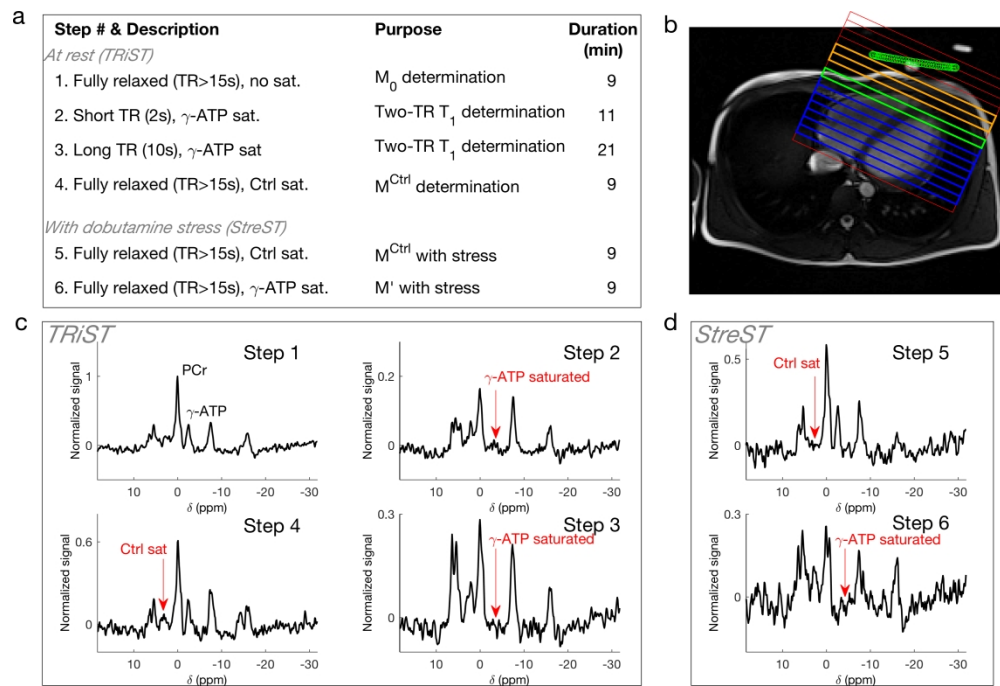


Figure 1. **a** Six-step StreST protocol (including TRiST as steps 1-4). **b** ^1H localiser with 1D CSI grid overlaid. The coil position is marked in green. Orange = Skeletal muscle, Blue = myocardium, green = Most anterior myocardial slice (coil slice distance < 60 mm). **c** Spectra acquired from the 4 steps of TRiST on a healthy, normal-weight subject. **d** Spectra acquired during dobutamine stress as part of the extension StreST measurement. In **c&d** signal is normalised to the PCr peak value in step 1.

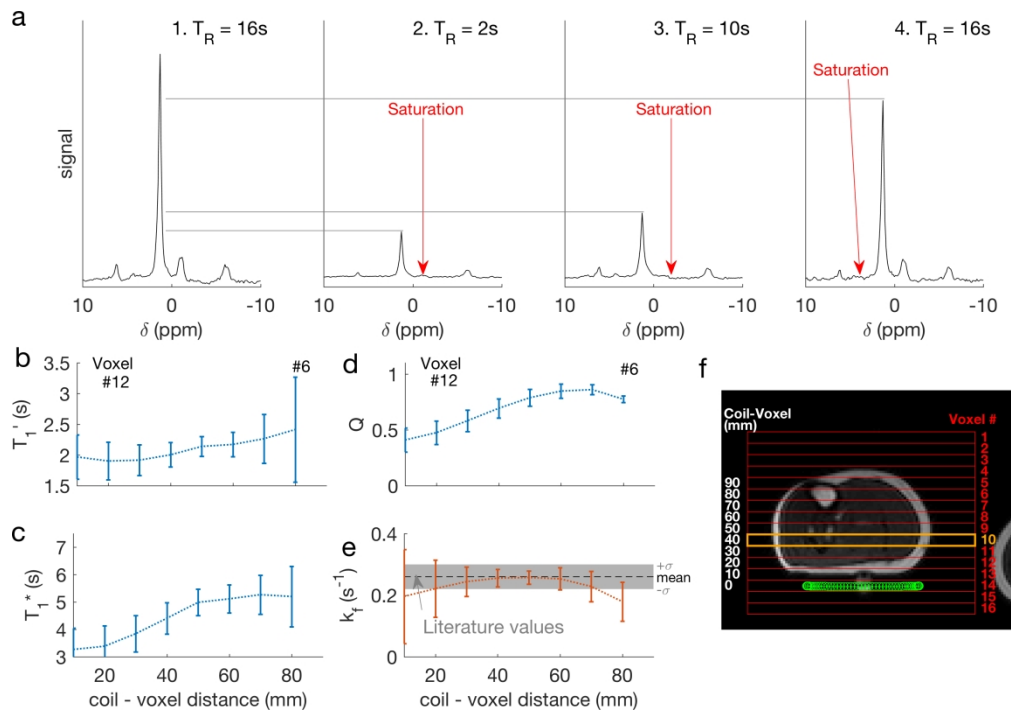


Figure 2. **a** Spectra from the four constituent scans of TRiST, showing the site of selective saturation, taken from a single slice in one subject (number 10, marked in orange in **f**). **b** Saturation-affected T_1 (T_1') for each subject in each slice, plotted as a function of distance from the coil. Error bars indicate (mean \pm SD). **c** shows the intrinsic T_1 (T_1^*), **d** the amount of direct PCr saturation (Q), **e** the k_f^{CK} , and **f** shows a localiser with a CSI grid overlaid (red), the slice plotted (orange), and the coil position (green).

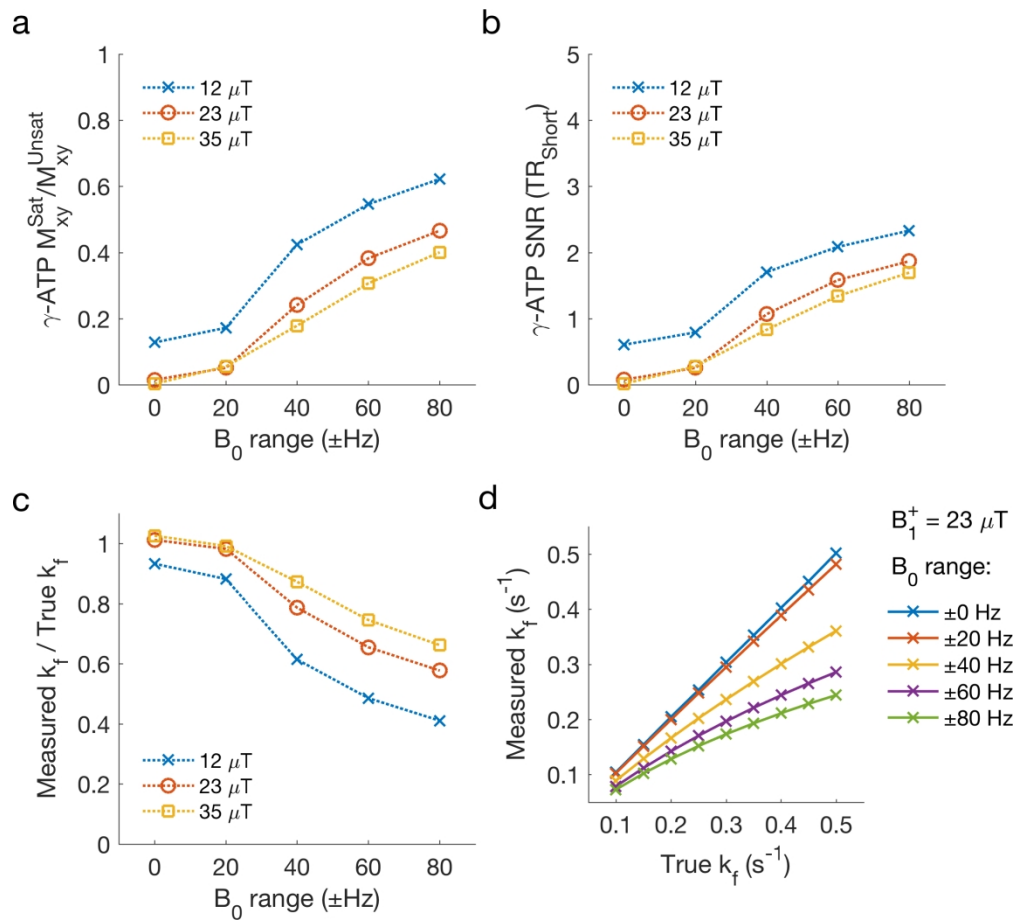


Figure 3. Simulated effect of respiration on the measurement of k_f^{CK} . **a** The ratio of γ -ATP transverse magnetisation in the presence of steady-state saturation (with respiration induced B_0 variation) versus the same sequence with no steady-state saturation. **b** The residual γ -ATP peak SNR. **c** The ratio of measured k_f^{CK} to true (simulation) k_f^{CK} . True $k_f^{CK} = 0.30 \text{ s}^{-1}$. **d** Measured k_f^{CK} in the presence of respiration induced B_0 variation at different values of true k_f^{CK} .

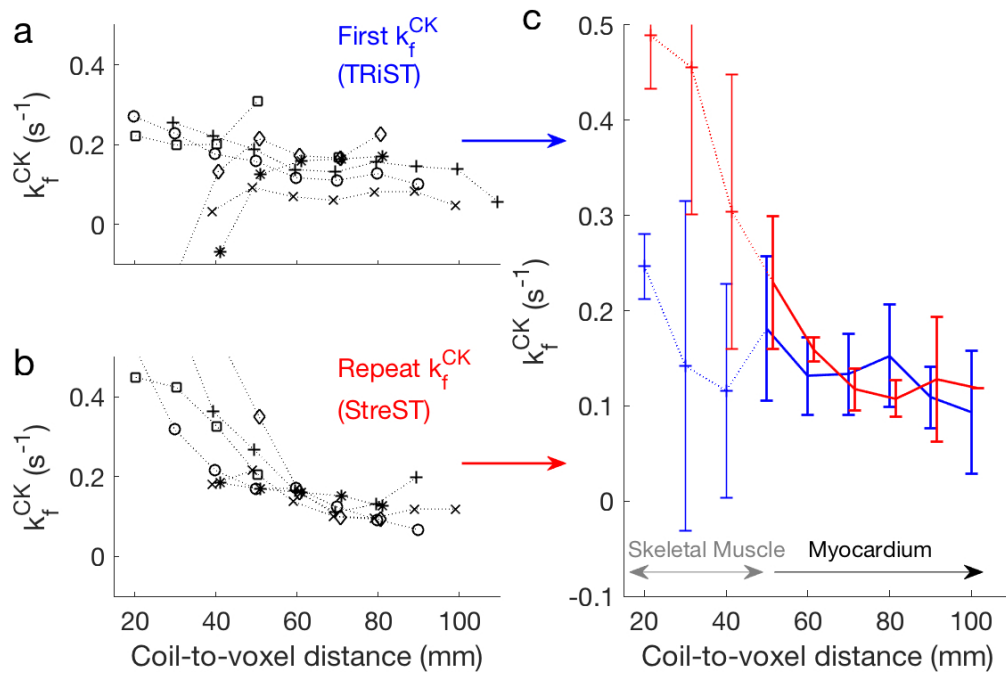


Figure 4. **a** TRiST and **b** StreST measured k_f^{CK} in the chest of six normal volunteers. Results are plotted as a function of coil-slice distance. StreST was performed without dobutamine stress for this validation study. Different markers denote different subjects. In **c** the inter-subject mean and standard deviation k_f^{CK} is shown for TRiST (blue: also 1st measurement of StreST) and the second measurement of StreST (red).

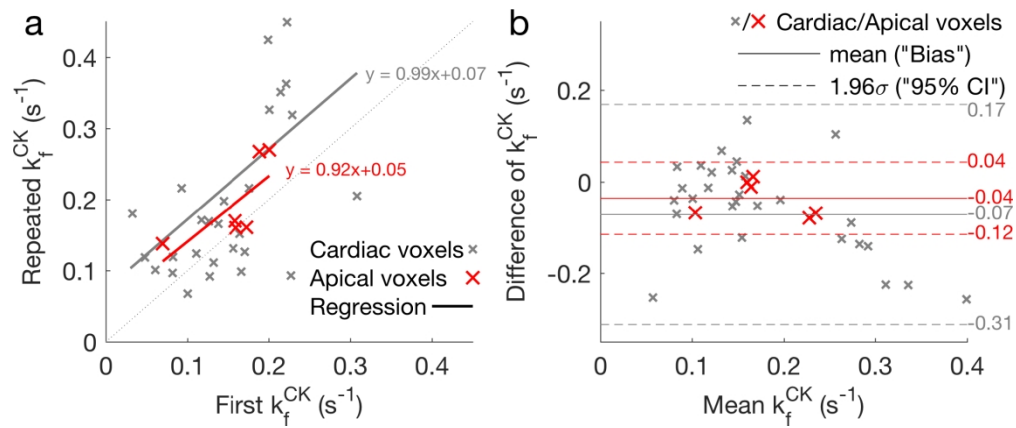


Figure 5. **a** Per-slice correlation plot of the two k_f^{CK} measurements in StreST (1st measurement equivalent to TRiST). All myocardial slices are shown, with the most apical cardiac slice for each subject shown in red. Results of linear regressions are also shown. **b** Bland-Altman comparison of the two k_f^{CK} measurements. The bias and 95% confidence intervals for each set of slices (all cardiac & apical) are marked.

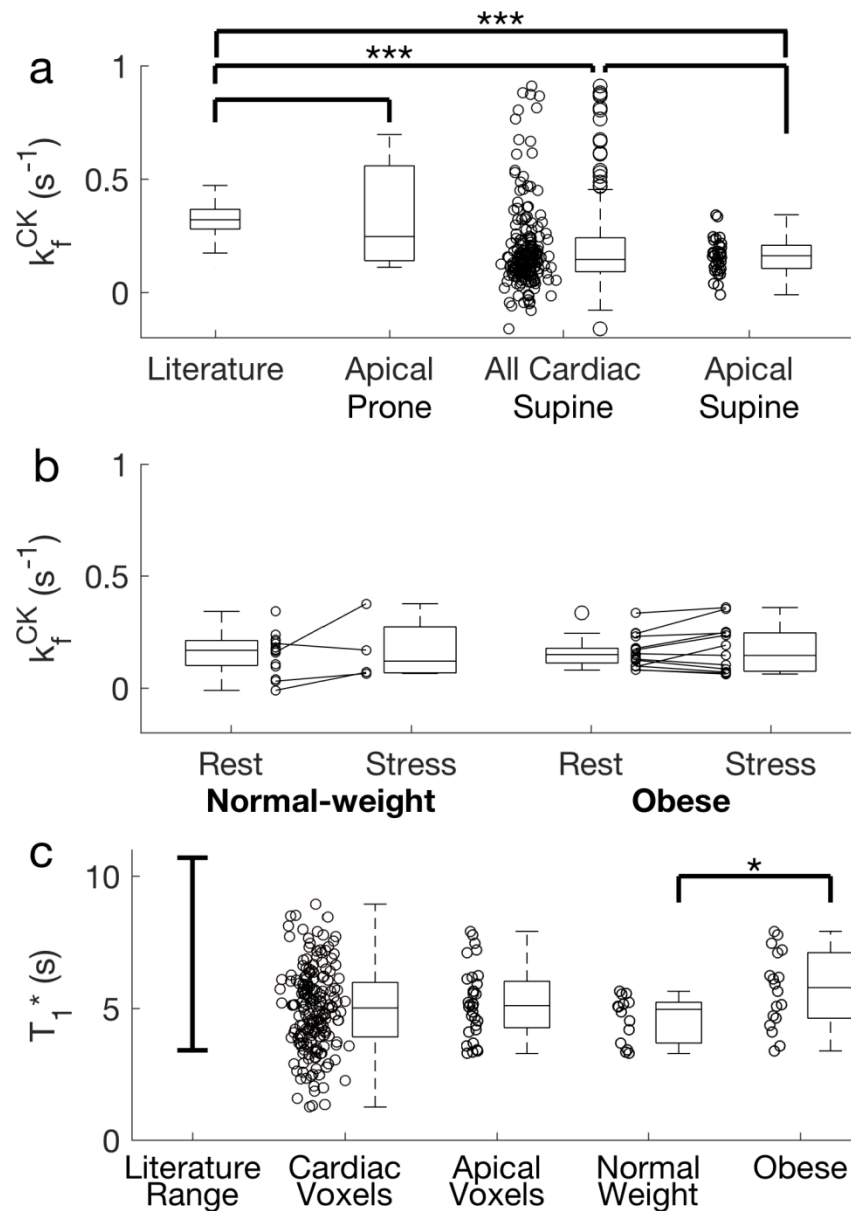
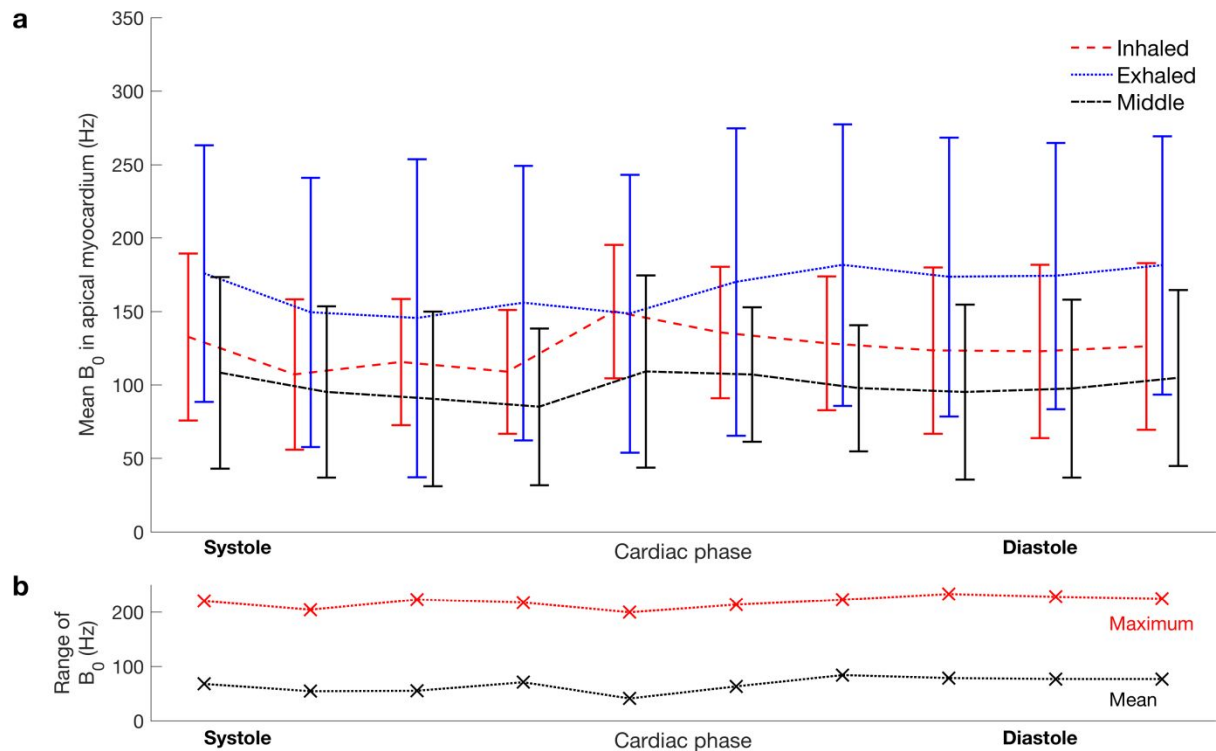


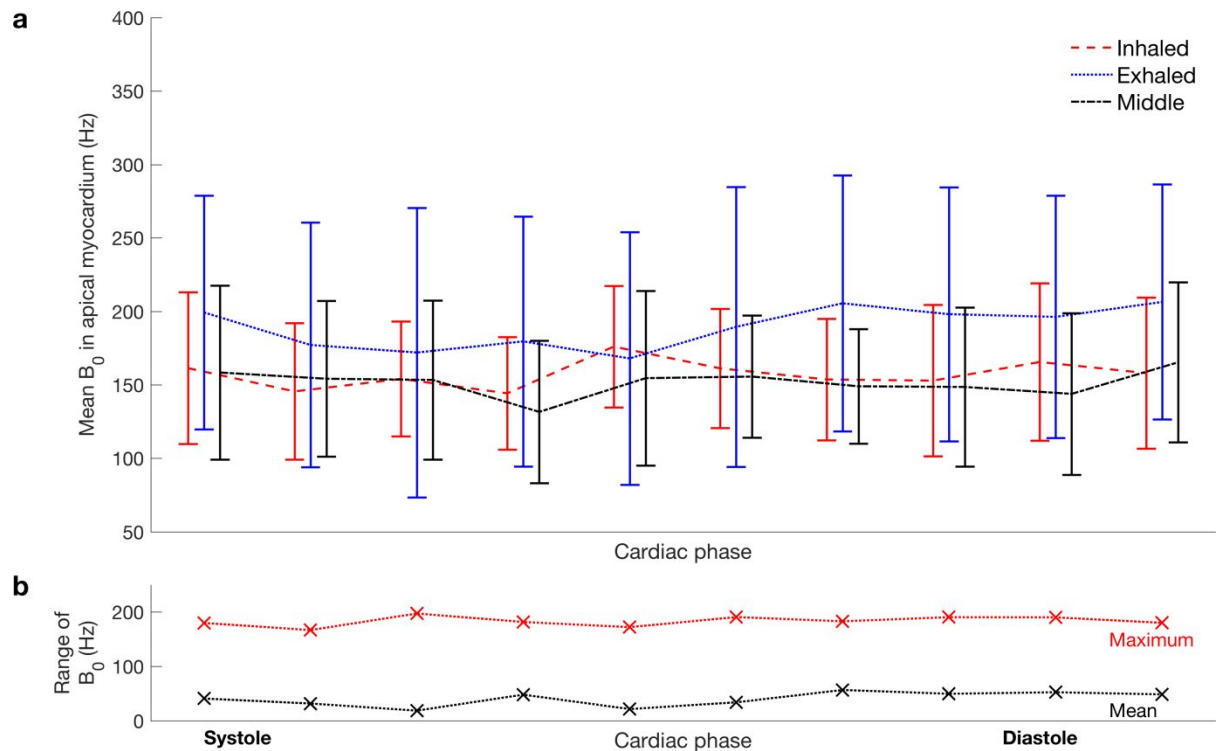
Figure 6. **a** The measured k_f^{CK} in all subjects undergoing the 4 scan TRiST measurement. Shown are the results from the prone validation, and all myocardial slices and anterior myocardial slices from supine scans.

b Rest and stress measurements from the selected slices of 34 normal-weight and obese volunteers.

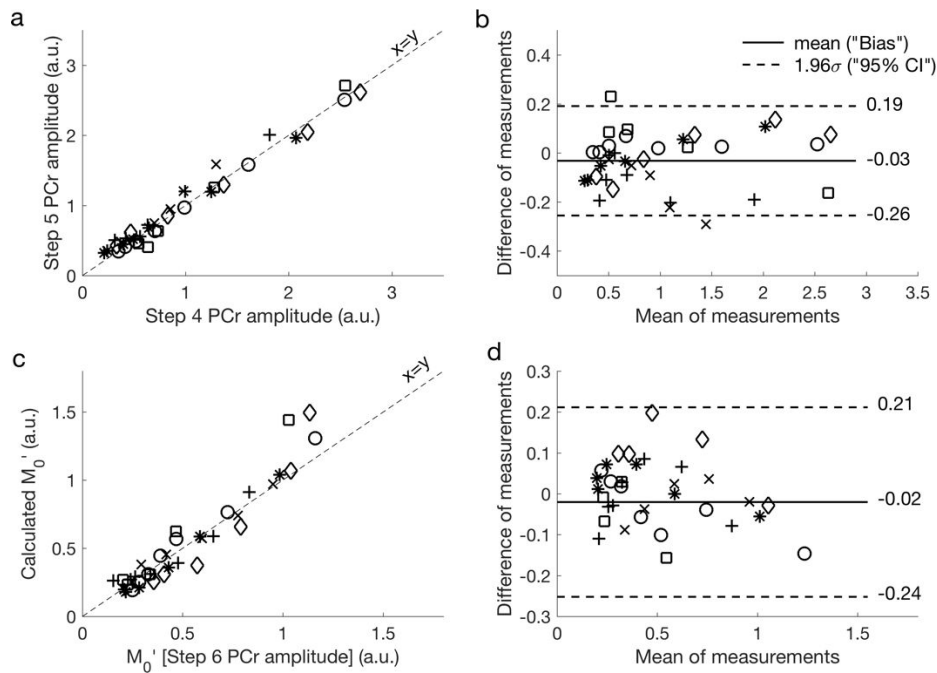
Negative values of k_f^{CK} are shown in this plot. Whilst negative k_f^{CK} values are not physically meaningful, they arise from noise entering into Equation 1. **c** Reported literature range of intrinsic T_1 (T_1^*)(7) compared to that measured in this study, for all cardiac slices, the most apical cardiac slices, and the apical cardiac slices from normal weight and obese subjects.



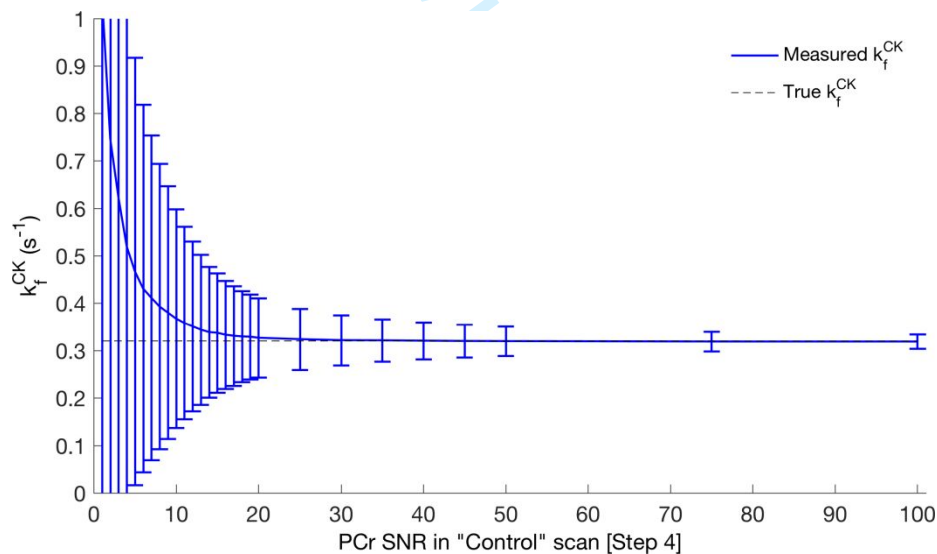
Supporting Figure 1 - B_0 variation in apical myocardium due to cardiac and respiratory motion in a **supine** position. **a** Mean(\pm SD) of per-voxel B_0 values in the apical myocardium of one subject. The B_0 field was measured at different phases of the cardiac cycle and at three respiratory positions (inhaled, exhaled and "middle"). **b** Range of B_0 values experienced at each cardiac phase across the three respiratory positions. The plot shows the range of the means (black) and the maximum range (red), corresponding to the first standard deviation of the distributions. In summary, the mean range of B_0 experienced in the apical myocardium due to cardiac motion is 34.3 Hz, and due to respiratory motion is 66.7 Hz. Values have been corrected for the lower gyromagnetic ratio of the phosphorus nucleus compared to the proton nucleus.



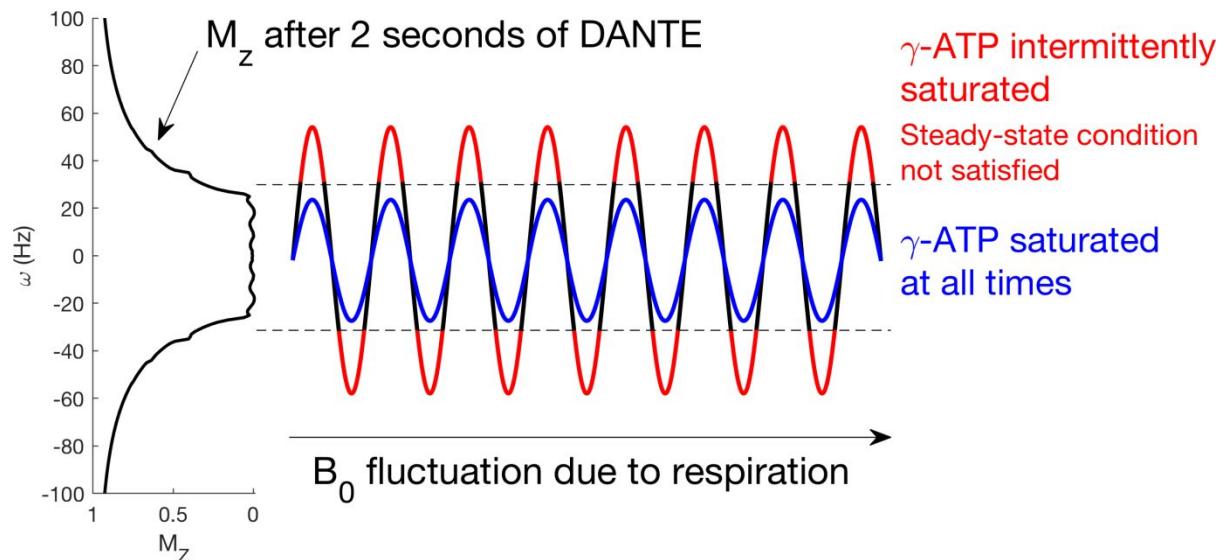
Supporting Figure 2 - B_0 variation in apical myocardium due to cardiac and respiratory motion in a **prone** position. **a** Mean(\pm SD) of per-voxel B_0 values in the apical myocardium of one subject. The B_0 field was measured at different phases of the cardiac cycle and at three respiratory positions (inhaled, exhaled and "middle"). **b** Range of B_0 values experienced at each cardiac phase across the three respiratory positions. The plot shows the range of the means (black) and the maximum range (red), corresponding to the first standard deviation of the distributions. In summary, the mean range of B_0 experienced in the apical myocardium due to cardiac motion is 34.6 Hz, and due to respiratory motion is 36.1Hz. Values have been corrected for the lower gyromagnetic ratio of the phosphorus nucleus compared to the proton nucleus.



Supporting Figure 3. Reproducibility of other parameters (validation scans). **a&b** Correlation and Bland-Altman plots of the fitted PCr amplitude of the 4th (M_0^{Ctrl} [TRiST]) and 5th (M_0^{Ctrl} [repeat]) scans. **c&d** Correlation and Bland-Altman plot of the calculated M_0' (from scans 2&3) and the directly measured M_0' (scan 6). The six different healthy subjects are shown with different marker shapes.



Supporting Figure 4 – Effect of signal-to-noise ratio (SNR) on the accuracy and precision of TRiST measured k_f^{CK} . Monte Carlo simulation of the TRiST measurement protocol was carried out at a range of different SNRs. The SNR was that of the PCr peak in the control scan (step 4 in Table 2). The plot was generated from 50000 repeats of the simulated measurement, with independent Gaussian noise added to each repeat for each SNR level. The plot shows the mean and standard deviation of the resulting measured k_f^{CK} .



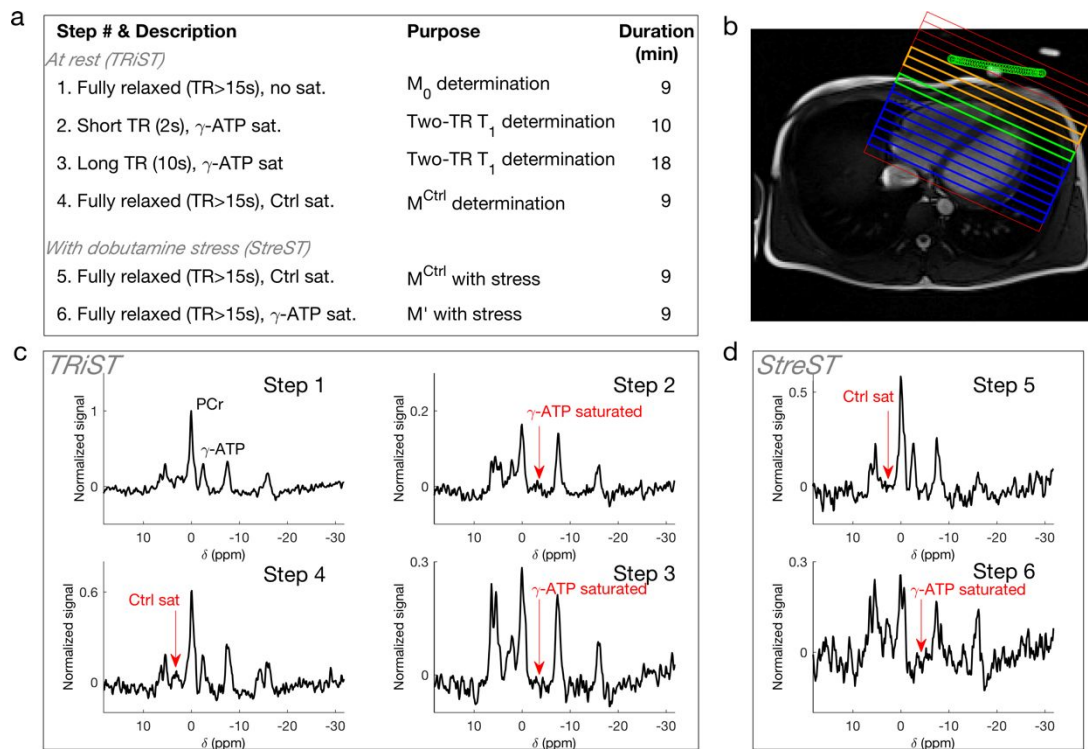
Supporting Figure 5 – Schematic of the effect of respiratory and cardiac induced B_0 fluctuation on steady-state saturation of γ -ATP. When fluctuation is low (blue line) the γ -ATP peak remains within the amplitude modulated broadened DANTE pulse's saturation band. The peak is therefore saturated at all times and the steady-state condition is fulfilled. If the fluctuation is large (black/red line) at some points the peak's position is shifted outside the saturation band and the steady-state saturation condition is violated.

Results Section	N	All cardiac slices			Apical slices	
		Slices	SNR	k_f^{CK} (s^{-1})	SNR	k_f^{CK} (s^{-1})
Validation of TRiST implementation Skeletal muscle (calf)	9	65	45±32	0.25±0.03	-	-
Validation of TRiST implementation Myocardium in prone position	10	29	18 ± 8	0.29±0.09	19 ± 5	0.32±0.15
Validation of TRiST implementation Myocardium in supine position	10	30	16 ± 9	0.15±0.10	17 ± 6	0.24±0.12
Validation of MRS measured k_f^{CK} by surgical biopsy	25	-	-	-	16 ± 6	0.21±0.10
Validation of the stress k_f^{CK} measurement (StreST) in healthy volunteers - 1 st Measurement	6	36	16 ± 9	0.14±0.08	15 ± 5	0.18±0.08
2 nd Measurement				0.22±0.14		
StreST in obese subjects and age-matched controls	34	209	14 ± 9	0.12±0.08	15±6	0.16±0.08
obese subjects – rest	18	-	-	-	-	0.16±0.07
obese subjects – stress	18	-	-	-	-	0.17±0.11
age-matched controls – rest	6	-	-	-	-	0.15±0.09
age-matched controls – stress	6	-	-	-	-	0.17±0.15

Supporting Table 1 – Summary of results. All values shown in this table are also contained in the results section text. Values are given as subject mean ± standard deviation. SNR is of the PCr peak in the control scan.

Localized rest and stress human cardiac creatine kinase reaction kinetics at 3 tesla

William T Clarke*, Mark A Peterzan, Jennifer J Rayner, Rana A Sayeed, Mario Petrou, George Krasopoulos, Hannah A Lake, Betty Raman, William D Watson, Pete Cox, Moritz J Hundertmark, Andrew P Apps, Craig A Lygate, Stefan Neubauer, Oliver J Rider and Christopher T Rodgers



Changes in the kinetics of the creatine kinase shuttle are sensitive markers of cardiac energetics but are typically measured at rest and in the prone position. This study aims to measure CK kinetics during pharmacological stress at 3T. We validate the MR measurement against biopsy assay of CK activity and evaluate normal ranges of stress k_f^{CK} in normal volunteers and obese patients. Our StreST protocol enables cardiac k_f^{CK} to be measured during dobutamine-induced stress.